

ELECTRODEPOSITION OF CERMETS

David William Snaith

In Candidacy for the Degree of

Master of Science

University of Aston in Birmingham

April 1970

S U M M A R Y

Modern engineering requirements are frequently near the useful limits of application of conventional materials. This has led to much, mainly empirical, work on the preparation of composites in which more than one conventional material is present. An example, known as a "cermet", consists of a ceramic in powder or fibre form imbedded in a metal matrix. Satisfactory improvements in properties can often be obtained by the application of a cermet coating onto a common metal and such coatings have been applied by electrodeposition techniques. Some of the factors underlying the cermet electrodeposition process have been investigated.

A ceramic particle in contact with an electrolyte solution will carry a charge. Under plating conditions such a charged particle may be transported by electrophoresis; the rate of transport for a given applied potential gradient would be determined by the charge carried by the particle. Measurements of this charge on particles of alumina, silicon carbide and chromium diboride have been made, in terms of the electrokinetic (zeta) potential, by a streaming potential method. Silicon carbide was chosen for a detailed study and the zeta potential on it was determined for various combinations and concentrations of copper sulphate and sulphuric acid and also of nickel sulphate and potassium sulphate.

Cermet materials, silicon carbide in copper and chromium diboride in copper, have been produced by electrodeposition and the distribution of ceramic particles through the cermet determined. The ceramic particle density in the cermet was related to the surface roughness, being highest where the surface was most rough and irregular.

It is suggested that the mechanism of deposition is a combination of electrophoretic transport of the particle through the double-layer at the cathode surface and of mechanical entrapment of the particle followed by keying into place by electrodeposited metal.

iv

Acknowledgements

The author wishes to thank Messrs. R. Ades and C. Moore of the Ipswich Civic College mathematics staff for their assistance with the interpretation of the experimental results and also Mr. P. D. Groves for encouragement and assistance during the course of this work.

CONTENTS.

Summary	Page	ii
Acknowledgements	"	iv
Chapter 1. Conventional materials, their properties and limitations	"	1
1.1 Wood	"	1
1.2 Ceramics	"	1
1.3 Metals	"	2
1.4 Composite materials	"	3
1.5 Metal/ceramic composites, "cermets"	"	7
Chapter 2. Electrodeposition of cermets: existing work	"	11
2.1 Surface coatings for wear and abrasion or for oxidation resistance	"	11
2.2 Preparation of materials for engineering applications	"	13
Chapter 3. Introduction to experimental	"	15
3.1 The mechanism of deposition of solid particles	"	15
3.2 Variable factors in the deposition process	"	16
3.3 Choice of ceramic and solution	"	17
Chapter 4. Theory underlying the experimental determination of the electrokinetic potential	"	19
4.1 The structure of the double layer	"	20
4.2 Electrokinetic phenomena	"	27
4.3 The effect of electrolytes on the	"	31

	double layer		
4.4	The effect of surface conductance and particle size on zeta potential measurement	Page	32
4.5	Values of terms used in the calculation of zeta potential by the Helmholtz-Smoluchowski equation	"	33
Chapter 5.	Experimental	"	34
5.1	Details of the streaming apparatus used in this work	"	34
5.2	Preparation of glassware	"	38
5.3	Materials used	"	39
5.4	Preparation of diaphragms	"	39
5.5	Preparation of solutions	"	40
5.6	Measurement of streaming potentials	"	40
5.7	Errors	"	41
Chapter 6.	Results and discussion of streaming potential measurements	"	42
6.1	Streaming results on alumina	"	42
6.2	Interpretation of streaming results of silicon carbide series SIC5 to SIC8 for Cu^{++} and H^+ as individual ions	"	43
6.3	Interpretation of the results of SIC5 for combinations of copper sulphate and sulphuric acid, for copper sulphate and for sulphuric acid	"	46
6.4	Interpretation of the results of SIC9 for combinations of nickel and potassium sulphates, for nickel sulphate and for potassium sulphate	"	47

6.5	Results of zeta potential measurements on silicon carbide using potassium chloride solutions, series SIC5 and SIC9	Page	48
6.6	Results of the investigation on chromium diboride using copper sulphate and sulphuric acid, series CRB2	"	49
6.7	Change in zeta potential with increase in ionic strength of the solution	"	49
Chapter 7.	Preparation and examination of cermet electrodeposits	"	61
7.1	Preparation of deposits	"	61
7.2	Electrophoretic transport of a charged particle in an electrolyte solution	"	62
7.3	Time to mechanically key a particle into an electroplated coating	"	65
7.4	Examination of cermet electrodeposits	"	66
Chapter 8.	Results and discussion of electro- deposition experiments	"	68
8.1	Distribution of ceramic through the metal matrix	"	68
8.2	The metal-ceramic boundary	"	69
8.3	The effect of ceramic inclusions on the structure of the matrix metal	"	70
8.4	Summary of the results of cermet electrodeposition	"	70
Chapter 9.	Conclusions	"	80
	Suggestions for future work	"	82

Appendix I.		Page	83
A1.1	Particle size. Justification of the use of silicon carbide, 280 grit, for streaming	"	83
A1.2	Conductance of the material	"	84
Appendix II.		"	85
A2.1	Calculation of the streaming potential from experimental results	"	85
A2.2	Variable terms in the Helmholtz- Smoluchowski equation	"	85
Appendix III.	Data layout for Calculation of zeta potentials	"	90
A3.1	Headings for each group of data	"	90
Appendix IV.	Statistical treatment of experimental results	"	92
Appendix V.	Experimental results	"	93
A5.1	Series SIC5	"	93
A5.2	Series SIC6	"	97
A5.3	Series SIC7	"	99
A5.4	Series SIC8	"	100
A5.5	Series SIC9	"	102
A5.6	Series CRB2	"	107
Appendix VI.	Calculation of maximum experimental error	"	108
Appendix VII.	Bibliography	"	112

Chapter 1. CONVENTIONAL MATERIALS, THEIR PROPERTIES AND LIMITATIONS.

The conventional engineering materials are wood, ceramics and metals. Synthetic plastics are also used but few of these find wide application without reinforcement.

1.1 Wood.

Wood has a low density and a high tensile strength in the direction of the grain but low strength at right angles to the grain. This weakness in one direction is not generally a great problem and can be largely overcome by laminating into plywood. The particular advantages of wood as an engineering material are due to its combination of strength, toughness, resilience, ease of shaping and joining and its light weight. These properties have made it particularly suitable for use in building construction, boatbuilding and the manufacture of airscrews and airframes: the latter two requiring considerable strength. Wood finds few other engineering applications, being unsatisfactory at much above room temperature and having little resistance to rot and chemical attack.

1.2 Ceramics.

Ceramics, compounds produced by combination of one or more metallic elements with one or more non-metallic elements, are characterised by hardness, high strength per unit weight, low density, imperviousness to heat, resistance to chemical attack and brittleness. This brittleness, in the case of natural materials such as stone or flint, makes them comparatively easy to shape by chipping. They also have a low coefficient of thermal expansion, and a high melting point, two factors which are particularly important when a structural material is used at elevated temperatures.

Ceramics are greatly weakened by the surface irregularities commonly present and by irregularities which occur at crystal boundaries. These irregularities can act as crack initiation centres. The low resistance to the propagation of such cracks (low work of fracture), gives the brittleness and hence potential weakness which is the traditional shortcoming of ceramics. Such crack initiation centres can be produced very easily in a ceramic by merely touching or heating it.^{1,2} As engineering materials ceramics have the additional disadvantage of being difficult to join except by the methods used in building construction.

Recent developments in the manufacture of ceramic components have overcome some traditional problems by performing the component from the metal or metalloid and then reacting it with its (gaseous) non-metal component at elevated temperature.

1.3 Metals.

The properties of metals are due to the nature of the bond between the metal atoms: by its nature the metallic bond is non-specific and non-directional; hence different metals can be readily joined or alloyed. Such structures are resistant to tension but have less resistance to shearing forces, thus explaining the ductility of metals. Most metals are naturally soft when pure; their strength is much increased by a high dislocation density, usually introduced by cold working. Deformation of such metal structures under stress occurs by movement of dislocations, hence the ease with which dislocations can be moved determines the hardness of a metal. Large foreign atoms in the structure can act as barriers to dislocation movement and hence increase the strength of the metal. The presence of microscopically fine particles of a solid foreign compound within the structure can similarly harden a metal, this being the principle of dispersion hardening of metals.

Metals and metal alloys find universal applications in engineering. Metals can readily be shaped by cutting, casting or by powder metallurgical techniques, the latter being particularly suitable for production of intricate shapes in expensive or very hard alloys.

The greatest disadvantages of metals as engineering materials are corrosion, leading to corrosion failure, and the fall in strength accompanying temperature increase: this fall in strength is often accompanied by corrosion which aggravates the weakening. Most metals in common use suffer from one or both of these disadvantages. The refractory metals such as molybdenum and niobium, which retain their strength at high temperatures, are very expensive and unalloyed are of little use except in an inert atmosphere as they oxidise at high temperature giving a volatile oxide. High temperature oxidation of metals can be greatly reduced by alloying, the best and most familiar examples being the alloying of iron to give the stainless steels.

1.4 Composite materials.

For many purposes the ideal material does not exist and for centuries attempts have been made to improve upon existing materials. Examples of such attempts include iron-bound wood, steel reinforced concrete and more recently glass fibre reinforced synthetic plastics. A particularly interesting example is paper pulp reinforced ice, in which the strength of ice was increased twenty times by freezing paper pulp into it.² The spread of cracks was blocked by the cellulose fibres.

1.4 - 1 The nature of composite materials.

These are materials combining the most desirable properties of two or more components. Many naturally occurring materials are composite in nature, for example in wood the cellulose fibres are bound in a matrix of lignin and in bone the protein collagen binds

together fibres of the mineral apatite. However a composite material sometimes has properties which are characteristic to itself and may bear little resemblance to those of its components. Glass fibre/plastic composites illustrate this particularly well as the mechanical properties of the composite product are very different from those of either component in its massive form.

The properties usually required in a composite material are either high strength and stiffness with light weight, high oxidation resistance and high strength at high temperature or resistance to abrasion. Basically the same materials are used to obtain products with each of these properties. Generally, and particularly in the aircraft industry, stiffness combined with lightness is more important than ultimate tensile strength as rigidity is of paramount importance. Applications of composite materials in nuclear engineering are a special case and will not be dealt with here.

In addition to improved mechanical properties it has been claimed that the incorporation of ceramic into metal, e.g. alumina into nickel, gives the metal enhanced high temperature oxidation resistance.^{3,4}

Ceramic can be incorporated as continuous or long fibres, whiskers (large single crystals of very great strength), or granules. These ceramic pieces are held in a matrix of suitable material. Greatest strength and stiffness can be obtained by ordered parallel alignment of long fibres as ordered packing permits the highest fibre density. As in wood, parallel fibre material has low strength at right angles to the direction of the fibres, although this problem can be largely overcome by laminating. Where abrasion resistance is required ceramic can be randomly incorporated as fine granules as generally an improvement in the strength of the material is not required.

1.4 - 2 Principles of the mechanism of reinforcement in composites having parallel fibres.

Fibre reinforcement is not directly concerned with restriction of dislocation movement although this could occur at high fibre densities. The basic concept is that if, in a two phase composite, stress is applied parallel to the fibres the strain will be equal in both fibre and matrix. Deformation of the matrix will transfer stress, by means of shear forces at the fibre-matrix interface, to the embedded high strength fibres. Hence when the material is under stress, the stress in the fibres is very much greater than that in the matrix. The contribution of the matrix material to the breaking strength of the composite is relatively small. If the length of the fibres is sufficient they should be constrained to take up the same deformation as the matrix over the greater portion of their length, thus effectively reinforcing the material. See fig. 1.1

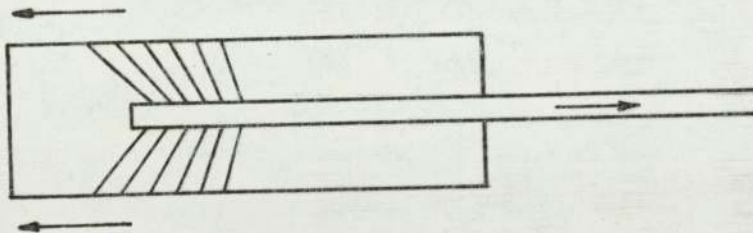


fig 1.1 Shear forces acting on a fibre near to its end.

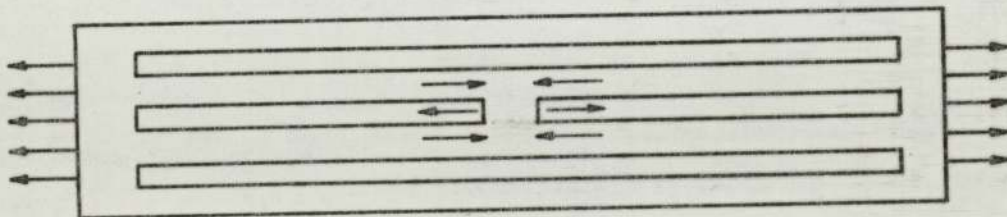


fig 1.2 Breakage of a reinforcing fibre.

When the central fibre breaks in the material under stress the two pieces of fibre tend to pull away from one another but are prevented from doing so by shear forces in the adhering matrix.

A good matrix material must be tough but plastic to transmit stress to the reinforcing fibres and to control cracks in the composite. The required properties are found in polymers and in soft metals such as copper, which being soft will not scratch the ceramic.

In service under high stress flawed fibres may break. This is probably unimportant as crack propagation will be prevented by the tough matrix material, particularly as it is most unlikely that all fibres which fail will fail in the same plane to give a smooth face on the break. To propagate a crack therefore some length of fibre must be pulled out of its matrix after breakage; work must be done by the applied force in pulling the fibres out against the forces holding them in the matrix. This work contributes to the total work of fracture of the material and it can not be attributed to the properties of either of the individual materials but is a true composite property, see fig 1.2.

In a high tensile strength composite the adhesion of the matrix to the fibre should be fairly low.⁵ This weak interface will mean that the composite will be weak at right angles to the fibre but its advantage is that a crack at right angles to the fibre can readily be deflected along the weak interface and hence be rendered harmless as far as desirable properties parallel to the fibres is concerned. However, under compressional or shear stress, buckling and splitting of the material is likely and to prevent this a strong interface is required. Adhesion of matrix to fibre will therefore always be a compromise.

When a fibre breaks under stress the part of the broken fibre close to the break will cease to support any load. A short distance away from the break the fibre will carry load as will an unbroken fibre near to its end. This is because as the fibre breaks the broken ends tend to pull away from each other but are restrained by the matrix material adhering to the fibre. Hence

the relaxing of the fibre is counteracted by the flow of the matrix parallel to the stress. Shear forces along the length of the fibre then reapply stress and this will occur even if all the fibres are broken or if many short fibres are used instead of long ones running right through the structure. Hence structures having multi-directional strength can be built using short fibres. These are less strong in any given direction than a structure having aligned fibres.

Because of their stiffness and strength per unit weight compared with other materials composite materials are used where these factors are of particular importance. Examples are carbon fibre/epoxy compressor blades in lightweight jet engines (Rolls Royce R.B 211 "Turbofan") and boron fibre/epoxy rotor blades for helicopters.

Two recent developments are (a) preparation of a whisker reinforced material by controlled solidification of certain eutectic alloys: part of the material is grown into parallel whiskers, the remainder becoming a matrix for the whiskers, an example is niobium carbide in niobium alloy, which retains high strength up to 1650°C (b) reinforced ceramic materials: solid state methods can cause fibrous growths inside a crystal of a solid ceramic material, an example being the growth, from the zirconium and calcium oxides present as impurities, of calcium zirconate filaments in solid magnesium oxide by suitable heat treatment. Doping of magnesium oxide has produced a random arrangement of filaments. Similarly doping of sapphire with rutile can produce filaments in the sapphire similar to those which reinforce natural star sapphire.² Still to be solved is the problem of alignment of the filaments necessary for maximum strength and stiffness.

1.5 Metal/ceramic composites, "cermets".

1.5 - 1 It is with ceramic reinforced metals, cermets, that this work is concerned. Cermets can be prepared in many different ways,^{6,7}

the most useful being:

(a) dispersion of ceramic particles throughout powdered matrix metal by mechanical action such as ball milling, followed by pressing into the required shape and sintering. Metals can be dispersion hardened in this way.

(b) coating of ceramic particles with a layer of metal powder held by a suitable binder, followed by pressing and sintering.

In these two methods the high compaction pressures necessary followed by the high temperatures used in sintering may cause severe damage to the ceramic. This may be unimportant in the case of dispersion hardening and in cermets for nuclear fuel element use.

(c) forming of the required final shape from ceramic powder or fibre followed by liquid metal infiltration under vacuum.

In a liquid state technique such as this, damage to the fibres is also possible as an extremely small amount of chemical interaction can result in a catastrophic weakening in surface sensitive ceramic fibres.^{8,9}

(d) electrodeposition methods. The ceramic in the form of granules or short fibres is suspended in a conventional plating bath, generally being maintained in suspension by mechanical stirring, air agitation or a combination of both methods. The object to be coated is hung in the bath and electroplating is carried out as for the metal alone. Cermet material can be plated onto a suitable former and then removed for use or it can be applied to a component as a wear resistant coating. Electrodeposition is particularly useful for coating intricate shapes such as gear wheels. The method also makes possible the application of an abrasion resistant cermet coating to an article which would be damaged by excessive heat.

1.5 - 2 Bonding between metal and ceramic in cermets.

Most methods for producing cermets involve high temperatures and the type of bonding which is found in such cermets falls into four general classes:

(a) a mechanical bond without evidence of chemical interaction, the metal being forced around the ceramic by pressure. An example is stainless steel reinforced with alumina: powder metallurgical techniques are used to produce components from a mixture of stainless steel and alumina powders.

(b) formation, by surface chemical action, of a third phase between the metal and the ceramic.

An example is boron fibre in a nickel matrix. Heating of an electroformed nickel/boron composite causes formation of a nickel boride layer between the boron and nickel and improves the strength of the composite: this may be because of better load transference from matrix to fibre.³²

Many metals commonly used in cermets do not wet the ceramic if heated in an inert atmosphere,¹⁰ but by modification of sintering conditions or addition of an alloying element wetting may be induced by mutual solubility with a third material. An example involving modification of sintering conditions is the preparation of chromium/alumina cermets, in the sintering of which slightly oxidising conditions are used giving a film of chromium^{III} oxide on the chromium. Chromium^{III} oxide is isomorphous with alumina (corundum)¹¹ and readily forms a solid solution with the alumina giving a strong bond.¹² An example of an alloying element which may be added to improve bonding is titanium.¹⁰ Titanium, loosely termed a detergent, has a high affinity for oxides and can react to form a third phase at the interface. (It has been said that it acts by reducing surface tension of the liquid metal)

This type of system has disadvantages, particularly that ceramic fibres may be seriously weakened by surface reaction giving rise to crack-initiation sites⁸ and that the fibre and matrix may react rapidly together, particularly at high temperatures, forming a thick boundary layer and seriously weakening the composite.³²

(c) grain boundary penetration with chemical reaction limited to the surface. This is very similar to (b).

(d) both phases are miscible. These are not true composites but tend towards solid solutions. Examples are chromium/tungsten and molybdenum/tungsten. It has been claimed that mutual solubility is an advantage.¹³

The bond formed in an electrodeposited cermet is probably largely mechanical, the non-conducting ceramic particles being held in place by the metal which has been electrodeposited around them. Bonds of the other types would probably not be present as they all require high temperatures in their formation.

High temperature oxidation resistance, resistance to mechanical abrasion and wear and also the mechanical properties of metals can be improved by the inclusion of a suitable second solid phase into a metal.^{1,3,4,12-34} Applications of electrodeposited composite materials fall into two main groups: those where surface coatings can be used on a conventional fabrication metal and those in which a component with particular mechanical properties is produced by electroforming.

2.1 Surface coatings for wear and abrasion or for oxidation resistance.

Where wear and abrasion or oxidation resistance is required a suitable surface coating on a common metal may often be the simplest and cheapest solution.²² Such a coating can readily be applied by electrodeposition. Much empirical work has been done in this field and the art has become well established: solid materials codeposited into metal films range from diamond, through common ceramic materials and lubricant particles to metal powders. Most of this work has involved alumina, silica and certain carbides and borides.

The powdered solid to be codeposited is dispersed in a plating bath suitable for plating the metal alone and is maintained in suspension by suitable agitation. Plating is carried out at a current density in the range suitable for plating the matrix metal.

2.1 - 1 Methods for obtaining an even dispersion of solid particles through the electrolyte have varied from simply stirring the solid into the bath to ball milling it in organic solvents followed by ball milling it in the electrolyte in order to get good wetting.^{3,4,16-25} For maintaining the particles in suspension mechanical stirring and/or air agitation have given consistently satisfactory results. Recirculation of the solution has been used,^{18,20} electrolyte/ceramic slurry being pumped from the bottom of the plating bath to the top, the ceramic settling onto the cathode

where it was occluded by electrodeposited metal.

2.1 - 2 Except in work using the settling technique, where particle size did not appear to be important, particle sizes used have generally been in the range up to about 5 microns diameter, although larger sizes have been used. When a solid with a wide size-range spread has been used it has been observed that predominantly fine particles, up to about 5 microns, are deposited, the larger particles remaining in suspension.^{24,25,35} It has been found difficult to deposit particles of larger size and this may be partially due to the increase in the mass/charge ratio with increase in particle size which would reduce any electrophoretic transport of the particles. When particles smaller than 1 micron were used some workers found that the particles were deposited as small agglomerates and not as discrete particles. They suggested that the use of very fine particles was of no advantage.^{3,16,23} However, particles as small as 0.02 microns are deposited satisfactorily in a widely used nickel/chromium plating process.³⁷

2.1 - 3 The proportion of particles in suspension, the "bath loading", was found to have a considerable effect on the proportion of ceramic found in the final product, the quantity occluded varying more or less logarithmically with bath loading at low loadings and linearly at higher loadings.^{19,21,24} Bath loadings of 10-100 g/l have been usual.^{3,19,21,24,36}

2.1 - 4 Plating baths used were those in general use for plating the metal, some being acidic and some alkaline. It has been claimed that for a high particle density in the deposit the solution pH should be kept low²⁰ and particularly so for lubricant particles, such as molybdenum disulphide and graphite which could not readily be codeposited with copper from a solution of pH above 4.^{21,24} When a copper/graphite deposit was made from such a bath

the deposit was poor and appeared to contain copper compounds as well as some graphite.²⁴ Another worker was unable to deposit alumina or silicon carbide from a copper sulphate/sulphuric acid bath or alumina from a Watts nickel bath at a pH of below 2 although satisfactory deposits of alumina in nickel were obtained in the pH range 2-5.¹⁹ However nickel/alumina deposits have been made at a pH of 1.5³ and copper/silicon carbide deposits at a pH of below 1, (this work).

In contrast, other workers claim that copper deposits containing a much higher proportion of ceramic particles can be obtained, for a given bath loading of ceramic, by using an alkaline cyanide solution instead of an acid sulphate bath. They claim that acid baths with good micro throwing power are less likely to give deposits high in ceramic as such baths will tend to deposit metal below the particle, thus lifting it away from the cathode surface.³⁶

2.1 - 5 Regarding the most suitable current density there is little information in the literature except for deposition of silica from alkaline copper cyanide solution.²¹ Generally a current density suitable for plating the matrix metal has been used. There is a case where different workers in the same laboratory have chosen different current densities as being best.³⁵ Periodic reversal of current has been recommended¹⁶ but has not been generally adopted as satisfactory electrodeposits can be produced without it.

2.2 Preparation of materials for engineering applications.

Maximum strength and stiffness is generally required when cermet materials are used for components in engineering. For maximum strength a high fibre density is necessary, as is precise parallel alignment of the fibres.^{33,38} Ideally the fibres should be continuous throughout the component, short lengths of fibre giving lower strength. For this reason materials having a random

arrangement of small ceramic particles or fibres are rarely suitable. An exception is where the particles are extremely fine and well dispersed in the metal and dispersion hardening is achieved.¹⁹ To obtain materials with the required physical structure special methods have been developed: these are based on continuous electrodeposition and filament winding in which method the filament is mechanically wound onto a mandrel immersed in the plating bath at the same time as metal is being electrodeposited.^{30,31,32} Nickel/boron, nickel/tungsten and nickel/carbon composites have been produced. In these processes the current density and filament winding rate have to be carefully chosen to prevent voids being left in the material.

Another process involving cermet electrodeposition is in the widely used process for producing a micro-porous chromium deposit over nickel (Udylite "Dur-Ni" process, Efco-Udylite "Nickel-Seal" process). In this process a non-conducting solid is codeposited in a suitable metal as a very thin layer on top of bright nickel. Chromium plating is then carried out by the usual methods. The presence of the solid non-conducting particles leads to micro-porosity in the chromium deposit.

3.1 The Mechanism of deposition of solid particles.

The mechanism of deposition of solid particles is not known for certain but theories have been advanced by various authors^{3,4,21,22}. The two extreme cases are (a) hydrodynamic transport of the particle to the cathode surface followed by occlusion of this particle by a build up of electrodeposited metal around it and (b) if the particle in contact with the plating solution became positively charged it would be moved towards the cathode by electrophoretic transport under plating conditions; once at the cathode surface it would be keyed into position by electrodeposited metal.

It is likely that the mechanism of deposition is a combination of these two factors. Electrophoresis cannot be the sole means of bringing up a particle to the cathode surface as in the bulk of the solution the rate of electrophoretic transport of the particle would be very small; approximately 5×10^{-5} cm sec⁻¹ under the usual plating potential gradient, (see 7.2). Electrophoretic transport may, however be the mechanism by which a positively charged particle traverses the double layer at the cathode. This double layer is in the order of 10^{-8} cm thick (see Appendix 1), and the potential gradient across it will be very much higher than that in the bulk of the solution (see Chapter 4).

Ultimately the solid particle will be held in place by a build up of metal around it but the crucial stage in the deposition process is the period while the particle is in contact with the cathode surface but has not been keyed into position by metal. This may be an appreciable time, approximately two minutes for a four micron particle at a smooth surface under optimum plating conditions in copper sulphate/sulphuric acid solution, (see 7.3). During this period some forces must hold the particle in place or

it would be swept away by the movement of the solution or knocked off the surface by impacts with particles in suspension before it became keyed into place by metal. Examples of forces which can restrain the particle at the surface are Van der Waals forces and, for a positively charged particle, the attraction for this charge by the negative cathode. That a positive charge on a particle is essential if the particle is to be occluded in a deposit has been suggested following the observation that deposition of lubricant particles was pH dependent, (see 2.1 - 4). This pH dependence has been explained by postulating that particles which in neutral solution may be uncharged or carry a negative charge can, under plating conditions in acid solution, adsorb hydrogen ions hence becoming positively charged.^{21,24} Attempts have been made to measure the zeta potential change on graphite with pH change but these have so far proved inconclusive.²⁴ In addition to these physical forces holding the particle onto the cathode surface mechanical factors such as the surface roughness of the metal and treeing at edges can assist retention of particles of solid: surface roughness because small particles (in the order of four microns) can lie in valleys between the peaks on many non-bright electroplated surfaces and are thus partially shielded from the moving solution and suspended solids which would otherwise tend to remove them. Because these particles are already partially surrounded by metal the time required to key them into position may be much reduced. At treed edges this mechanical entrapment can be very great indeed, such parts of the deposit being very high in non-metal content but very porous and brittle, (see 7.4).

3.2 Variable factors in the deposition process.

The variable factors thought to be important in the deposition process are the metallic element deposited, the composition of the plating solution including its pH, the roughness of the metal surface,

the nature, physical state and size of the ceramic and the sign and magnitude of the charge on the ceramic. Of these variables it is known that solution composition and sign and magnitude of charge on the ceramic in contact with it are related and it was this relationship which was chosen for study. The other variables were to be kept constant: particles of a given constant size could be deposited with a particular metal from a specified plating solution which, under given operating conditions, will give a reproducible surface roughness.

3.3 Choice of ceramic and solution.

The choice of ceramic and solution was silicon carbide and a copper sulphate/sulphuric acid electrolyte. The charge on the particle was measured as the electrokinetic potential (zeta potential, ζ). Silicon carbide, supplied by the Carborundum Company, was chosen primarily because of its chemical inertness, initial exploratory work using alumina (corundum) having indicated that a chemically inert material was to be preferred. Further advantages were its ready availability in a consistent state of purity and in a range of suitable particle sizes each size having very little size scatter from that stated. The wide use of silicon carbide as an abrasive also recommended it for this work as it could readily be used in wear resistant composite electrodeposits. A copper sulphate/sulphuric acid plating solution was chosen because this combination finds wide use in electroplating and electroforming practice and also because, having only two constituents, it is reasonably simple to study.

In addition to the streaming potential measurements made on silicon carbide in contact with copper sulphate/sulphuric acid solutions a replicate series of determinations was carried out in which the solution was nickel sulphate/potassium sulphate. This combination was chosen because, compared with the previous

solution, the cations only are different. This solution made possible the determination of the effects of combinations of different 2:1 and 2:2 electrolytes on the zeta potential of silicon carbide.

Some measurements were made of the effect of the copper sulphate/sulphuric acid electrolyte on the zeta potential on chromium diboride. Chromium diboride was chosen for this study because, unlike silicon carbide which contains group IV atoms only, it contains transitional and group III atoms. Like silicon carbide it is chemically inert.

Chapter 4. THEORY UNDERLYING THE EXPERIMENTAL DETERMINATION
OF THE ELECTROKINETIC POTENTIAL.

It was first observed by F. Reuss in 1809 that when a potential difference was applied between electrodes placed on either side of a plug of moist clay or sand a flow of water was observed through the plug. A porous plug or diaphragm is actually a mass of fine capillaries and it was subsequently found that this process, known as electroosmosis, also took place in capillary tubes, singly or in groups (Quincke 1861).

The first quantitative measurements (Wiedmann 1852, 1856) showed that the electroosmotic pressure for a given diaphragm material was proportional to the applied emf. It was shown by Quincke in 1861 that the direction of flow of the liquid in electroosmosis was due to the existence of electrically charged layers of opposite sign at the boundary between the liquid and the material of the diaphragm: the application of a potential difference must result in the displacement of the charged layers relative to each other and since the liquid is free to move, whereas the diaphragm is not, a flow of liquid occurs; the direction of flow will depend on whether the liquid carries a net positive or negative charge. This interpretation of electroosmosis also accounted for the fact that if a liquid is forced through a porous diaphragm or other capillary system, a potential difference, known as the streaming potential, is set up between the two ends (Quincke 1859). This process can be regarded as the reverse of electroosmosis. Two other observed electrokinetic effects were electrophoresis (F. Reuss, 1809) in which suspended particles are moved under the influence of an applied potential difference, and sedimentation potential (E. Dorn, 1880) which is set up when suspended particles are set in motion under the influence of gravity. The concept of the existence of oppositely charged layers

20

at the solid liquid boundary was extended by Helmholtz³⁹ who suggested that an electrical double layer is generally formed at the boundary between two phases.

4.1 The structure of the double layer.

4.1 - 1 The model due to Helmholtz.

Helmholtz saw the double layer at the plane interface as a layer of excess ions or electrons on the solid phase and an equivalent amount of oppositely charged ions in the solution. The ions in the solution were situated at a minimum distance δ from the surface corresponding to the particular ionic radius. This model resembled a charged capacitor with a plate separation δ . The potential of this capacitor should decrease linearly with distance x from the surface:

$$\frac{d\psi}{dx} = -4\pi h$$

where ψ is the electrostatic potential, h is the charge density and x is the distance from the surface. In practice it was found that this theory was not adequate to explain the capacity of the double layer as the capacitance of a phase boundary itself depends upon h and thus upon the concentration of the electrolytic solution. It is a useful approximation in concentrated solution (where the effects of surface conductance are negligible).

See fig. 4.1.

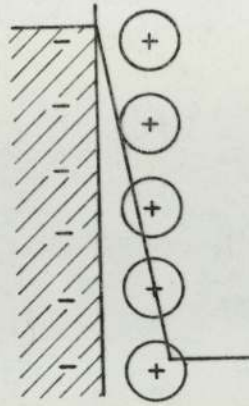


fig 4.1 Helmholtz's model of the double layer.

4.1 - 2 The model due to Gouy and Chapman.

A considerable improvement on this theory was obtained by Gouy⁴⁰ and by Chapman⁴¹ who considered the charge on the solution side of the double layer not as a surface charge but as a spatial charge with a statistical distribution. As the whole double layer must be neutral the surface charge must be equal and opposite to the spatial charge existing in the solution part of the double layer:

$$h_0 = - \int_0^{\infty} \rho \, dx$$

where h_0 is the surface charge density and ρ the space charge density. However the values of the capacitance of the double layer calculated by using Gouy and Chapman's theory are up to ten times larger than the experimentally determined values,⁴² indicating that the Gouy-Chapman theory of the double layer also is inadequate. The principal reason for failure of the Gouy-Chapman approach was the assumption that the ions were point charges

so that the ionic charge distribution could be continuous up to the solid surface. This allowed a large space charge to arise very near to the solid surface leading to an anomalously large calculated capacitance for the double layer. See fig. 4.2.

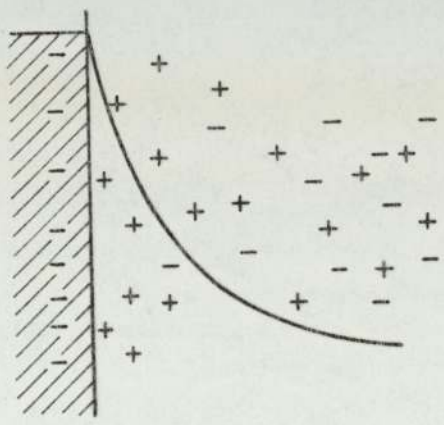


fig 4.2 Gouy and Chapman's model of the double layer.

Gouy recognised the importance of a distance of closest approach, a , for ions of a finite size and this concept was treated in detail by Stern³⁴ (see also D.C.Grahame⁴⁴).

4.1 - 3 The model due to Stern.

Stern considered that if the ions have a finite size (e.g. their crystallographic or, better, their primary hydration (8) radii, r) the continuous charge distribution must be cut off at $r = a$ and hence the potential/distance relation near the surface is discontinuous, the minimum distance of approach being r where r is the particular ionic radius. Stern also assumed that certain ions could be specifically adsorbed onto the solid surface and he was thus able to explain the dependence of potential on the composition of the solution in terms of this specific ion adsorption. He postulated a "plane of closest approach" and assumed that this was

the same for anions and cations. The total potential drop can be resolved into two components: a drop across the diffuse portion of the double layer ψ_s which may be calculated by the use of Gouy-Chapman theory and a linear drop across the compact "Helmholtz" layer $\psi_0 - \psi_s$ See fig. 4.3.

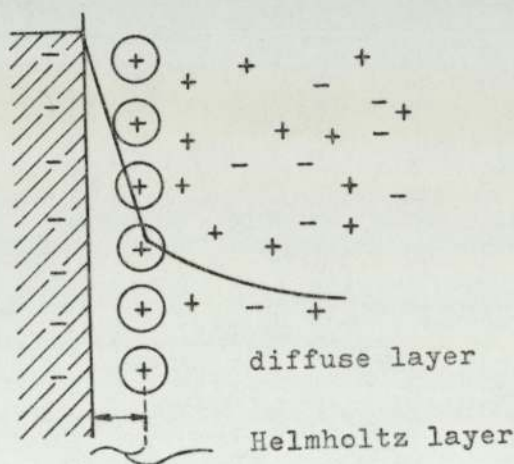


fig 4.3 Stern's model of the double layer

The total capacitance C_0 is made up of the constant capacitance C_1 of the compact layer and the concentration dependent capacitance C_2 of the diffuse layer. These capacitances are in series, so

$$\frac{1}{C_0} = \frac{1}{C_1} + \frac{1}{C_2}$$

As the concentration of electrolyte in the solution is increased the number of ions present will increase. In the Helmholtz layer there is dynamic equilibrium between the ions and the solid surface; an increase in concentration, although it will increase the number of ions in this adsorbed layer, will not have a very great effect. This may be compared with the case of gas adsorption on a surface where coverage is almost complete. In contrast to this the concentration of ions in the diffuse Gouy-Chapman layer will be

considerably increased. Capacitance of the double layer depends upon the charge per unit area of the layer and hence upon the ionic concentration per unit area. The capacitance of the Gouy-Chapman diffuse layer will thus be increased considerably more than that of the Helmholtz adsorption layer by an increase in electrolyte concentration. Hence in very dilute solutions, where $C_1 \gg C_2$, $C_0 \approx C_2$ and in concentrated solutions, where $C_2 \gg C_1$, $C_0 \approx C_1$ (i.e. the value of the smaller capacity contribution mainly determines the overall value of the double layer capacity C_0 .) The total capacitance is governed largely by the capacitance of the compact adsorption layer C_1 and can never exceed C_1 . The capacitance C_2 of the diffuse portion of the double layer exerts only a minor effect. The excessively large capacitances of the Gouy-Chapman theory therefore cannot arise.

4.1 - 4 The model due to Grahame.

Stern's model has been modified by Grahame⁴⁴ who defined three regions of potential drop: from the solid surface to the layer of specifically adsorbed anions, the inner plane of closest approach; from this layer to the inner limit of the diffuse (Gouy) layer, the outer layer of closest approach, and across the diffuse layer. Specific adsorption was located in the inner layer of closest approach. He thus distinguished between an inner and outer "Helmholtz " layer, the respective thicknesses of which are determined by the radii of anions and hydrated cations. The diffuse layer is adjacent to the outer Helmholtz layer. (See fig. 4.4)

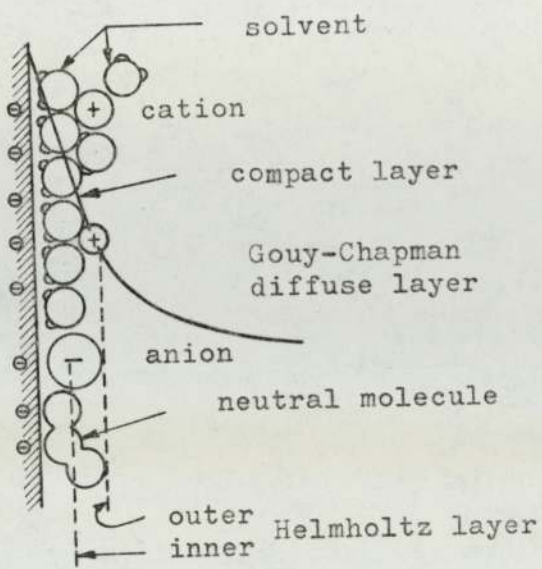


fig 4.4 The double layer with reactant adsorption.

Working with a mercury surface Grahame observed that hydrated cations with a structure resembling an inert gas (i.e. nontransitional elements) are not specifically adsorbed. The hydrate envelopes of such ions remain intact and their interaction with the charged metallic surface is purely electrostatic. Conversely most anions are specifically adsorbed with loss of most or all of their hydration envelope. This may be explained: an ion in solution, being charged, will have an attraction for one end of water dipoles and will attract to itself a layer of adsorbed water. The stability of this solvation envelope depends upon the attraction of the ion for the water molecule being sufficiently strong to overcome the attraction of water molecules for each other, i.e. to break the weakly-bonded tetrahedral lattice of water. Big ions (mainly anions) are not strongly hydrated but small ions with high charge density will have the greatest attraction for water molecules; these ions are mainly cations, F^- being an exception. Grahame found that by using sodium fluoride solutions no specific adsorption of anions or

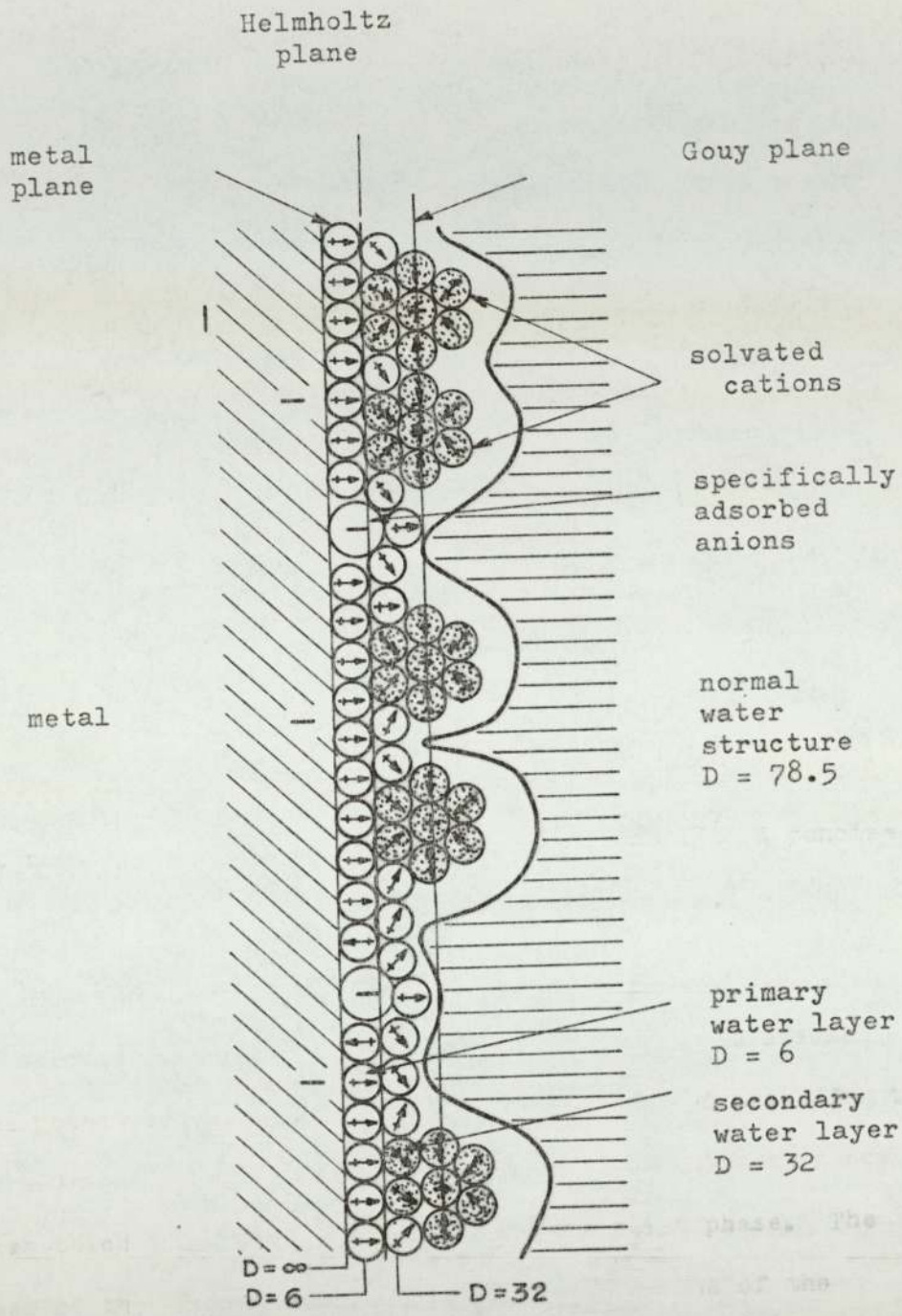


fig 4.5 Solvent adsorption model of the double-layer according to Devanathan, Bockris and Müller, (Proc. Roy. Soc. (1963), A274, 55.)

cations took place.^{44,45}

4.1 - 5 A recent theory⁴⁶ suggests that the adsorbed cations with their primary hydration shells remain outside a layer of strongly oriented adsorbed solvent dipoles shown, in fig. 4.5, at a cathodic surface. Specifically adsorbed anions are regarded as being able to penetrate the inner solvent layer. This theory has the advantage of taking into account in a realistic way the (hitherto neglected) presence of adsorbed solvent by showing that the cathodic capacity is determined mainly by the inner layer of orientated water dipoles and is therefore largely independent of cation radius, i.e. the adsorbed water determines the thickness of the cation layer and hence the associated capacity.

4.2 Electrokinetic phenomena.

Following the discovery of electrokinetic phenomena quantitative treatments of these phenomena were given by several workers, notably Helmholtz³⁹ and later Smoluchowski.⁴⁷ A concise rederivation of their equations is given by G. Kortüm.⁴⁸

4.2 - 1 Electroosmosis.

To calculate the electroosmotic rate of flow it is assumed that the potential in the double layer is distributed according to the Stern-Grahame model and that a layer of liquid at most a few molecules thick adheres to the surface of the solid phase. The thickness of this layer is less than $\frac{1}{K}$, the thickness of the double layer, and the rate of flow within it is equal to zero (laminar flow). N.B. $\frac{1}{K}$ is analogous to the radius of the ionic atmosphere as given by the Debye - Hückel theory and this may be taken here as the thickness of the double layer. A glide plane is formed between the fixed layer and the moving liquid. This plane is situated within either the Helmholtz layer or the Gouy-

Chapman layer. The Helmholtz-Smoluchowski equation for electroosmosis is

$$v = \frac{DE\xi}{4\pi\eta_0}$$

(see Appendix VI), where D is the dielectric coefficient of the moving liquid, E is the applied external field in volts cm⁻¹, η_0 is the coefficient of viscosity in poises and ξ is the "electrokinetic potential" in volts i.e. the value of the potential ψ in the glide plane. This is identical to the value of the "zeta" potential between the parallel "plates" of the Helmholtz model of the double layer. v is the rate of flow outside the double layer and will be greater than the velocity within the double layer; therefore the Helmholtz-Smoluchowski equation will only be valid when the radius of the pore or capillary is large in comparison with $\frac{1}{K}$. This is true under most practical conditions except when the capillaries are very small as in semi-permeable membranes.⁴⁸

If the glide plane is situated not in the Gouy-Chapman layer but in the Helmholtz layer then D and η_0 can no longer be regarded as constant⁴⁶ and the Helmholtz-Smoluchowski equation must be replaced by

$$v = \frac{E}{4\pi} \int \frac{\rho}{\eta_0} d\psi$$

(where ρ is the spatial charge density) which cannot at present be evaluated owing to lack of data concerning viscosities and dielectric constants within the Helmholtz layer.⁴⁹

4.2 - 2 Streaming potential.

If a liquid is forced through a capillary system a potential difference, known as the streaming potential, can be detected between the ends of the capillary system. This process can be

considered as the opposite to electroosmosis.

4.2 - 2 - 1 Mechanism of streaming potential generation.

Two alternative mechanisms for the way in which streaming potential is generated have been suggested. The more familiar mechanism is that one section of the double layer remains fixed to the solid phase and when the streaming liquid flows past the surface of the solid phase it will carry away with it the ions (mainly of the same charge) lying outside the glide plane. This leads to a convection current which produces opposite charges on the ends of the capillary system. As electrolyte solutions are conducting, a stationary state is reached in which the pd due to ionic migration balances the streaming potential generated as described above. The magnitude of the streaming potential thus depends upon the specific conductance K' of the solution. In calculations it is again assumed that the tube walls are non-conducting and that the only path for the conduction current is in the bulk of the solution, that the capillary radius r is large in comparison to the thickness of the double layer $\frac{1}{K}$ and that surface conductance^{47,51} may be neglected. (Surface conductance may be ascribed to the fact that in the double layer the ionic concentration is greater than that in the bulk of the solution and hence the double layer has a higher conductance than the bulk of the solution. Surface conductance is appreciable in dilute solutions.) The alternative mechanism is suggested by Lewis:⁵⁰ under streaming conditions the ionic atmosphere at the solid surface is distorted or polarised with respect to the solid material. The measured emf represents a massive polarisation of all the permanent and induced dipoles in the system.

The Helmholtz-Smoluchowski equation for streaming potential is

$$E = \frac{\zeta P D}{4 \pi \eta_0 K'}$$

where P is the pressure difference between the ends of the capillary system and E is the measured potential difference. It has been shown that ζ , for a given material, when determined by streaming potential measurements is identical to that determined by electroosmosis.^{52,53,54.}

4.2 - 3 Electrophoresis.

In electrophoresis solid particles suspended in the liquid are set in motion by an electric field whilst the liquid remains at rest. This may be contrasted to electroosmosis in which the liquid moves past a stationary solid phase under the influence of an electric field. The presence of the electrical double layer at the phase boundary affects the relative motion of the two phases in both cases.

The equation $v = \frac{D E \zeta}{4 \pi \eta_0}$ as used for electroosmosis can

therefore be directly applied to calculations of electrophoretic velocity. As before it is assumed that the thickness of the double layer is small compared to the size of the particle, which can be of any shape but must be an electrical insulator. It must also be assumed that the convection conductance of the particles is so small that it does not interfere with the homogeneous external field. N.B. if the convection conductance is large, the counter-emf produced at the particle interface will reduce the electrophoretic velocity.

As the sign and magnitude of the zeta potential on a particle is constant in a given electrolytic solution, irrespective of the method used to determine it, it is evident that a knowledge of the zeta potential on a particle will give an indication of how rapidly the particle will move in an applied electric field.

4.3 The effect of electrolytes on the double layer.

That the presence of a certain minimum amount of electrolyte is essential for the stability of hydrophobic colloids may be demonstrated by removal of electrolyte from such a colloid by electro dialysis. When electrolyte concentration falls below a certain minimum value the colloidal particles cease to repel one another, coagulate and precipitate.⁵⁵

Addition of small amounts of electrolyte to a suspension may cause either an increase or decrease in the ζ potential on the particles but at moderate concentrations ($> 2 \times 10^{-5}$ g ion/l) the ζ potential decreases with increasing concentration of electrolyte and at a rate which increases with the valency of the counterion.^{48,54} It has similarly been shown⁵⁶ that for various electrolytes the zeta potential on glass (negative sign) varies linearly with the logarithm of the concentration at low electrolyte concentrations ($< 10^{-7}$ g ions/l):

$$\zeta = A - B \log C$$

Zeta potential is thus almost independent of salt concentration when the salt concentration is very low, particularly if the salt has univalent ions, but may change sign at high concentrations. This is shown in fig. 4.6.

4.4 The effect of surface conductance and particle size on zeta

potential measurement.

Although the existence of surface conductance has long been

known, its effect on the measured value of the zeta potential

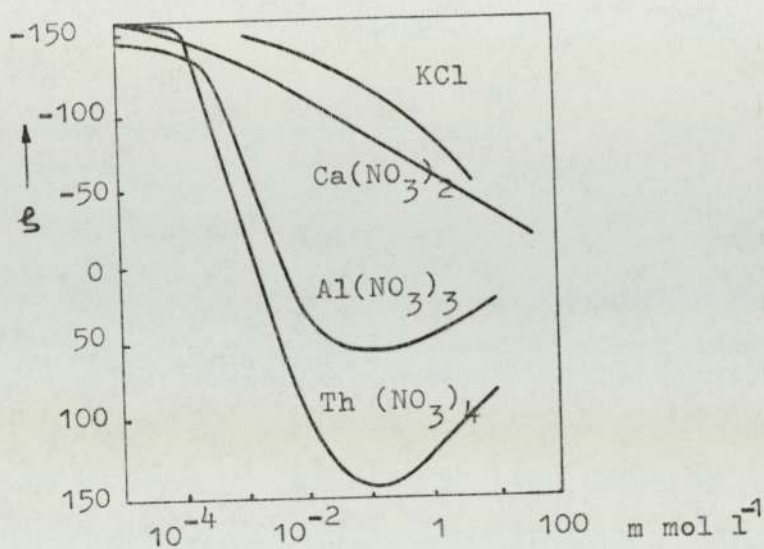


fig 4.6 Zeta potentials at glass surfaces as a function of concentration for various electrolytes.

These observations can be explained in terms of the diffuse double layer. The thickness of the double layer is practically unaffected by small additions of salts but contracts significantly in the presence of larger additions⁵⁷ (see 4.1 - 3). Rutgers and deSmet⁵⁶ demonstrated that the rate of decrease in the zeta potential increases with increasing valency of counter-ions, in agreement with the Schulze-Hardy rule.^{58,59} Mathematical explanations for these observations have been given.⁶⁰ Different counterions possessing the same valency may, however, exert different effects which, by analogy with the reversal of the sign of the zeta potential in the presence of large additions of salts, can be attributed to the specific adsorption effects inherent in the Stern-Grahame concept of the double layer.

4.4 The effect of surface conductance and particle size on zeta potential measurement.

Although the existence of surface conductance had long been recognised its effect on the measured value of the zeta potential

was apparently ignored until the work of Fairbrother & Mastin⁶¹ and of Briggs.⁶² These workers, particularly Briggs, showed that the density of packing of a diaphragm directly affected the measured value of the streaming potential and ascribed this to surface conductance in the diaphragm.

Because of surface conductance the effective conductance K'_s of the streaming liquid in the diaphragm is greater than the conductance K'_b of the liquid in bulk and in accurate determinations of zeta potential K'_s must be used. Methods have been suggested for the determination of K'_s .^{61,62}

As a change in the density of packing of a diaphragm will give a change in K'_s and hence in the observed E/P value for the diaphragm it is necessary always to have the same solids to volume ratio of a given material if comparative results are required. Similarly, if non-compressible granular materials are being used, it is necessary to use a constant size of particle: reducing the particle size will increase the surface area/volume ratio, the effects of surface conductance will become more significant and K'_s will increase.

It has been claimed that accurate values of the zeta potential from streaming data can only be obtained for coarse granular materials;^{50,63} Neale⁶³ claimed that the particle size must be such that the pore size is at least ten times greater than the thickness of the double layer.

4.5 Values of the terms used in the calculation of zeta potential by the Helmholtz-Smoluchowski equation.

In all calculations the value of K' used was the bulk conductance K'_b . The values of the dielectric constant and coefficient of viscosity were those of the pure solvent at the temperature of streaming. Detailed justification for the use of these values is given in appendix 1.

If streaming potentials are to be measured the apparatus must have facilities for holding a granular or fibrous sample as a diaphragm, for applying hydrostatic pressure to this diaphragm, for measurement of this pressure and for measuring the streaming potential which is generated. That part of the apparatus which comprises the diaphragm holder and the electrodes used for the detection of the streaming potential is known as the "streaming cell" or "cell".

The simplest design of cell is a horizontal tube in which the diaphragm is held between perforated metal discs which also act as electrodes for detecting the streaming potential. Silver, gold and platinum have been used. The potential difference set up is measured using a suitable potentiometer circuit. Such cells suffer from several disadvantages, the principal ones being channelling of the streaming liquid over the top of the diaphragm, loss of fine particles of the diaphragm material past the metal discs and polarisation and non-reversibility of the metal electrodes. Considerable improvements in the mounting of the diaphragm and for measuring the streaming potential are possible and a considerably improved cell design was introduced by Lewis⁵⁰ who used a vertically mounted diaphragm together with opposed saturated calomel half-cells⁶⁴ for detection of his streaming potential. This cell formed the basis of the design used in this work.

5.1 Details of the streaming apparatus used in this work.

The apparatus is shown diagrammatically in figs. 5.1 and 5.2.

5.1 - 1 Streaming cell.

The cell was mounted vertically, the diaphragm being retained by a mat of filter paper supported on a perforated platinum disc.

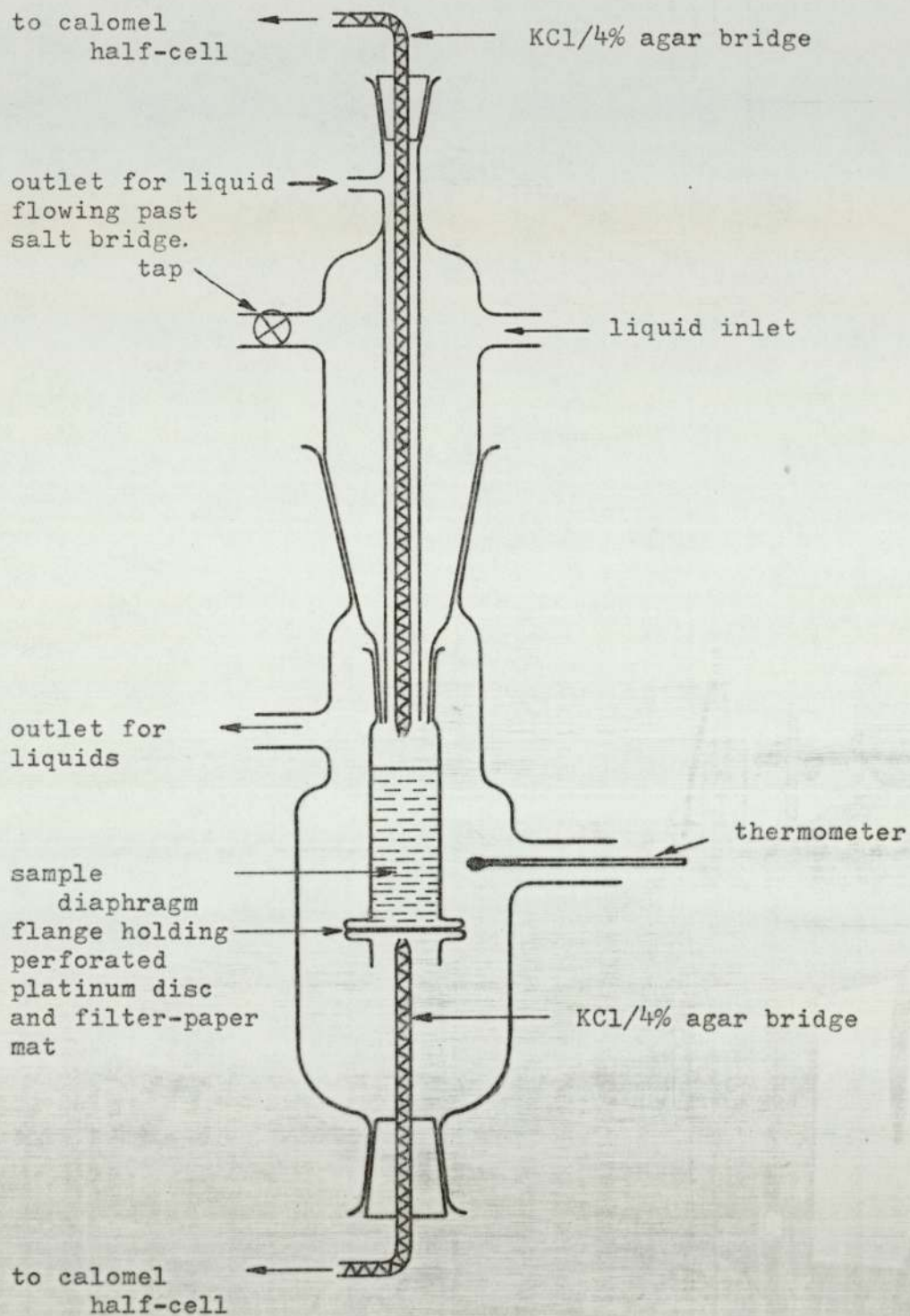


fig 5.1 Schematic diagram of the streaming potential cell.

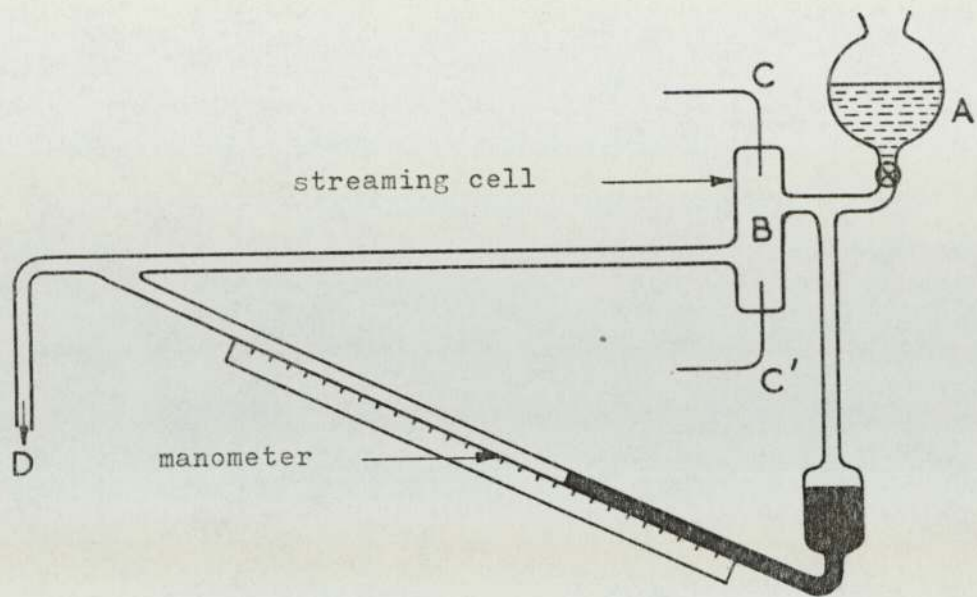


fig 5.2(a) Schematic diagram of streaming apparatus.

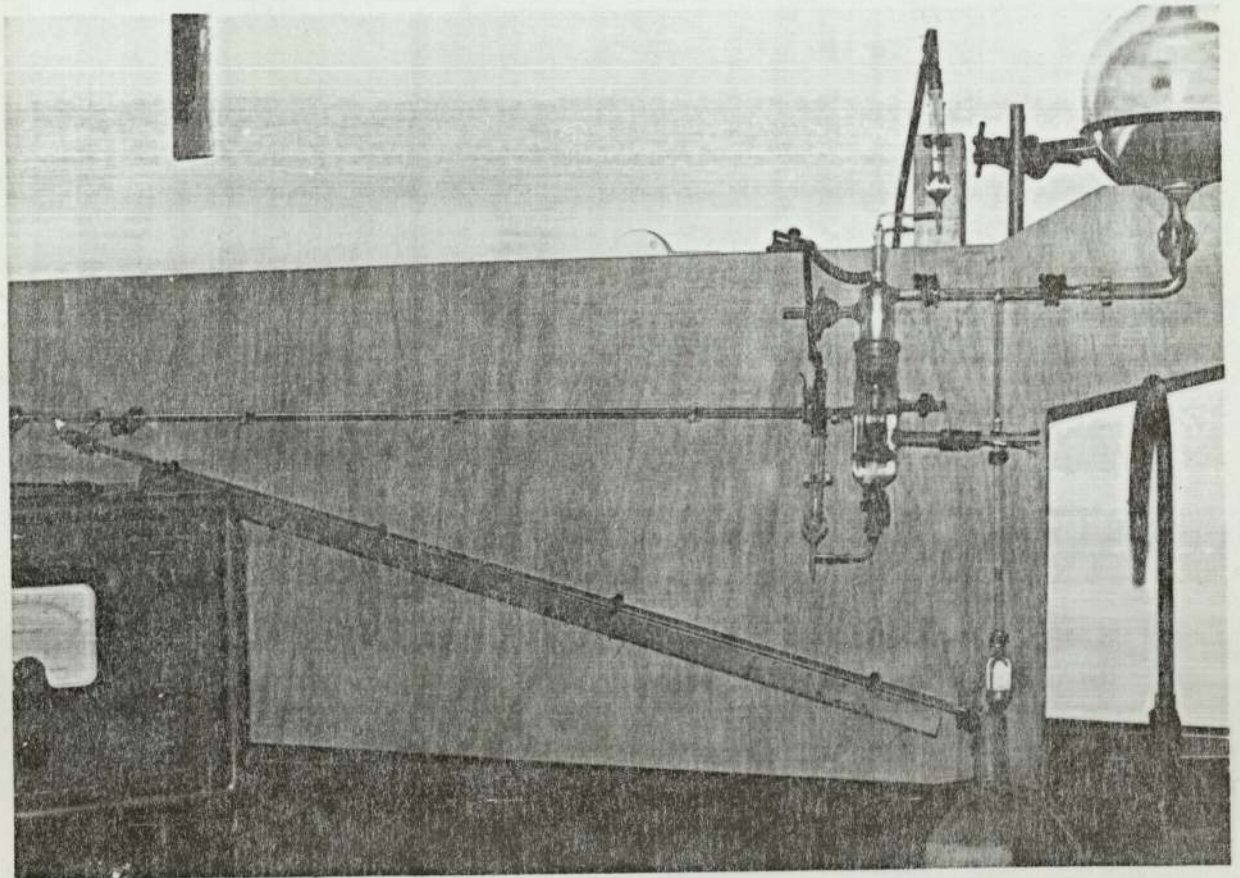


fig 5.2(b) Photograph of streaming apparatus.

The mat and platinum disc were held between glass flanges. The mat material, Whatman 541 paper, was chosen in preference to other materials because it was resistant to acid solutions, consistent in quality and had a pore size small enough (3.4-5.0 microns) to retain the diaphragm material without clogging.⁶⁵ The streaming potential developed across the mat in the absence of the silicon carbide diaphragm was constant at 5% of the value obtained in the presence of the diaphragm.

5.1 - 2 Detection of streaming potential.

The streaming potential was detected by the use of two opposed saturated calomel half-cells connected, by means of 4% agar/saturated KCl probes ending in fine capillaries, into the cell at opposite ends of the diaphragm. Provision was made for a reverse flow of liquid to waste past the upper probe during streaming to prevent contamination of the streaming liquid with KCl leached from the probe.⁵⁰ However in practice it was found that variation of the reverse flow significantly altered the measured streaming potential; reverse flow was not used. Although the distance of the detecting probes from the diaphragm does not affect the measured value of the streaming potential⁵⁰ the sensitivity of the detecting circuit decreases with increasing probe separation. In order to obtain maximum sensitivity the probe ends were mounted as close to the diaphragm as possible.

5.1 - 3 Measurement of streaming potential.

Streaming potential was measured using a vibrating reed electrometer ("Vibron 33B", EIL Ltd.). This instrument gave less precise readings (± 0.1 mv.) at low pd than could have been obtained using a potentiometer but because it was direct-reading it was much more convenient to use than a potentiometer. Connection of the calomel half-cells to the electrometer was made using shielded wire to prevent fluctuation caused by stray currents.

5.1 - 4 Hydrostatic pressure between the ends of the diaphragm.

This was obtained by applying suction to the lower end of the cell. The suction was controlled by variation of an air bleed in the system. Sudden fluctuations of pressure were minimised by the presence of a large capacity reservoir in the vacuum line. The pressure difference between the ends of the diaphragm was measured using a sensitive mercury manometer. A conventional manometer with two vertical arms was unsuitable as small pressure changes could not be read off precisely from it. A six-fold increase in sensitivity was obtained by using a manometer with one inclined arm of fine-bore (approx. 1 mm diam.) tubing and one vertical arm of wide-bore (approx. 2 cm diam.) tubing giving a ratio of small-bore: wide-bore of approx. 400:1. The manometer is shown diagrammatically in fig. 5.1. When suction was applied to end D of the manometer mercury rose up the inclined arm of the manometer and fell in the vertical arm but because of the difference in tube diameters the rise in the sloping arm was very much greater than the fall in the vertical arm. As the pressure was measured in the usual way almost the entire pressure difference was indicated by the rise in the inclined arm; hence any pressure change gave almost double the vertical movement in the sloping arm that would have been obtained using two arms of equal bore. Also as the fine-bore tube was inclined at approximately 30° to the horizontal the column moved about 3 cm. for each 1 cm. of vertical height. An increase in sensitivity of approximately six times was achieved by the use of this manometer design. This manometer was calibrated against a conventional manometer.

5.2 Preparation of glassware.

New glassware has a significant amount of leachable soluble salts and alkali in its surface. To prevent contamination of

streaming solutions with electrolyte leached from the glass all glass parts carrying the streaming solution to the diaphragm were soaked for several days in 50% sulphuric acid to remove all alkali and were then steamed out for several hours to remove all traces of water-soluble salts.

5.3 Materials used.

Corundum, α alumina, was used for initial exploratory work. It was used "as supplied" and also after being boiled in conductance water.

Silicon carbide was used for the main investigation. The grade used for streaming was 280 grit, average particle size 37 microns, supplied by the Carborundum Company Ltd. Streaming measurements were made on this material "as supplied" and also after various pretreatment processes: (a) boiling in water to remove any soluble impurities, (b) soaking in 1 normal sulphuric acid (the concentration usually used in an acid sulphate copper bath) followed by boiling in water to remove all traces of electrolyte and (c) successively soaking in concentrated nitric, hydrofluoric and sulphuric acids⁶⁶ followed by boiling in water to remove all traces of electrolyte. This last treatment was not of great interest as in practical use the material would be most unlikely to get a pretreatment of this nature before being used in deposition work. The results obtained using untreated "as supplied" material and that boiled in water or soaked in sulphuric acid were indistinguishable and subsequent diaphragms were prepared from "as supplied" material.

Chromium diboride was used for a short investigation. This material, size range 53 - 63 microns was used "as supplied". The supplier was Borax Consolidated.

5.4 Preparation of diaphragms.

Any fines present in the powder were separated by repeated

sedimentation of the powder in water. The diaphragm was then prepared from this powder by sedimentation, under gravity, through conductance water in the diaphragm tube to form a column.

5.5 Preparation of solutions.

All solutions were made up using conductance water prepared by deionisation of distilled water. A three-stage deionisation system was used comprising cationic, anionic and mixed cationic/anionic exchange resins. The water produced was stored in a steamed-out aspirator fitted with a carbon dioxide trap. All solutions were prepared using analytical grade reagents.

Streaming potential measurements were carried out using solutions of copper sulphate, sulphuric acid and mixtures of copper sulphate and sulphuric acid. Stock solutions of copper sulphate, sulphuric acid and copper sulphate/sulphuric acid mixtures were prepared and appropriately diluted for streaming. The concentration of Cu^{++} and H^+ solutions used for streaming were 0.000008, 0.000032, 0.000128 and 0.000512 g ion/l.

$CuSO_4/H_2SO_4$ mixtures were prepared having ionic proportions $Cu^{++} : H^+$ 1: $\frac{1}{8}$, 1: $\frac{1}{4}$, 1: $\frac{1}{2}$, 1:1, $\frac{1}{2}$:1, $\frac{1}{4}$:1, and $\frac{1}{8}$:1. For streaming these solutions were diluted as for the single-compound solutions, e.g. a $Cu^{++} : H^+$ 1: $\frac{1}{2}$ mixture would be diluted for streaming such that the copper ion concentrations were from 0.000008 to 0.000512 g ion/l.

5.6 Measurement of streaming potentials.

To determine the streaming potential for a given solution and diaphragm the streaming solution was made to travel, under pressure, from the reservoir A and vertically downwards through the diaphragm B. The streaming potential was detected by the two saturated calomel half cells C and C' connected to the measuring

electrometer. The pressure applied was varied in 1 cm steps from 1 to 12 cm of mercury and at each pressure the steady-state streaming potential was recorded. This procedure was repeated twice in order that statistical scatter limits could be determined. Hydrostatic pressure, for forcing the streaming liquid through the diaphragm, was obtained, as described in 5.1 - 4, by applying suction from a vacuum pump to the used-solution outlet D.

When a streaming solution was changed all traces of this solution were removed from the apparatus by repeated washing; the diaphragm was thoroughly flushed by streaming for about 15 minutes at a pressure of approximately 8 cm of mercury. It was noted that after about one minute of flushing a constant streaming potential was obtained.

The temperature of the streaming solution was measured in every case by using a thermometer inserted into the streaming cell. The specific bulk conductance of each solution was measured using a dip cell and a Wayne Kerr Universal A.C. bridge.

5.7 Errors.

In this work a number of variables had to be measured, each involving error. An estimate of the total experimental error was desirable and to this end an estimate of the maximum error in the measurement of each variable was essential. These estimates are given in appendix VI; where the percentage could have more than one value the highest was taken.

The maximum experimental error was $\pm 20\%$

5.1 Streaming results on alumina, Al_2O_3 .

The streaming activity of alumina was not found to be consistent and reproducible results could not be obtained. Variation of streaming activity was so great that

MEASUREMENTS.

The zeta potential was calculated as shown in appendix II for the various combinations of solutions and diaphragm materials.

Typical examples of the results of the preliminary exploratory work on alumina (corundum) are shown graphically in figs. 6.1, 6.2 and 6.3. Results of the work on silicon carbide and chromium diboride are shown graphically as K'_b vs ζ graphs, K'_b being on a logarithmic scale and ζ on a linear scale. The results in tabular form, together with the limits of variation for 95% confidence are given in appendix V. There is a considerable amount of scatter in the experimental results. It has been stated that various workers have found that the streaming activity of a given diaphragm decreased with successive measurements. This effect was observed throughout the present work and has given rise, to some extent, to the wide variation limits in the experimental data. (see Appendix VI.)

The reference number of each streaming run was chosen such that it would act as an immediate "finger print" for the particular diaphragm and streaming solution used. For example, when copper sulphate solution was streamed through the fifth diaphragm of silicon carbide the reference number S1C5/CU was given. Full details regarding the assignment of reference numbers is given in appendix III.

6.1 Streaming results on alumina, Al_2O_3 .

The streaming activity of alumina was not found to be constant with time and reproducible results could not be obtained. Variation of streaming activity was so great that frequently the polarity of the streaming cell and hence the sign of the zeta potential reversed while under a constant

applied streaming pressure.

Two possible explanations for these observations can be made:

- (a) the presence of surface contaminants on the alumina could cause the zeta potential to be initially incorrect. With prolonged streaming such contaminants would be removed and the true zeta potential of the solid observed;
- (b) alumina may be affected by water. If its surface reacts even slightly with water the result could be the formation of a hydrated oxide. In water and more particularly in solutions of acids and alkalies this hydrated oxide could dissolve giving a loss of the surface atoms of the solid. Instability could be caused by the presence of the ions dissolved from the alumina surface.

In addition to these difficulties the early work was complicated by the use, as recommended by Lewis⁵⁰ and others, of coarse granular powders. Diaphragms made from these powders had a high permeability and hence allowed a large liquid flow which could not readily be maintained for an extended period in this apparatus. It is therefore possible that equilibrium was not always achieved between solid and solution. Furthermore the low permeability of the mat material used to retain the diaphragm relative to that of the diaphragm itself could have given errors.

Because of uncertainty regarding the reliability of experimental results the alumina was replaced by silicon carbide as the diaphragm material after the exploratory stages of the project. (See 5.3.)

6.2 Interpretation of streaming results of silicon carbide series

S1C5 to S1C8 for Cu^{++} and H^+ as individual ions.

The experimental results were plotted on log/linear graph paper, figs. 6.4 and 6.5. In all of these determinations the zeta potentials are negative but all become less negative with increase in K'_b . It was not possible to draw straight lines for all of the experimental sequences SIC5 to SIC8 but if the upper, straight-line, portion of the curves is considered it is evident that although the actual calculated values of zeta potential vary from sequence to sequence the rate at which the zeta potential changes with $\log K'_b$ is similar.

6.2 - 1 SIC6/CU is slightly different from SIC6/CUB and SIC6/CUC but the latter two are indistinguishable, SIC6/CUB was carried out one hour after SIC6/CU but SIC6/CUC was carried out after the diaphragm had been allowed to stand in contact with water overnight (16 hours). These results suggest that after soaking in the aqueous solution for about one hour the diaphragm had reached a steady state.

6.2 - 2 SIC7/CU is very similar to SIC6/CU suggesting that soaking of the diaphragm in water has very much the same effect as soaking it in 1N H_2SO_4 . This treatment with sulphuric acid prior to use in streaming was therefore considered unnecessary.

6.2 - 3 SIC8/CU is similar to SIC6/CU and SIC7/CU but it has a greater change of zeta potential with K'_b than have the latter two.

6.2 - 4 SIC8/CUB is very similar to SIC6/CU and to SIC7/CU and its upper linear portion has a gradient similar to that of SIC5/CU.

6.2 - 5 SIC6/H is indistinguishable from SIC6/CUB and SIC6/CUC and similarly SIC8/H is indistinguishable from SIC8/CUB.

6.2 - 6 The graphs have been drawn within the limits of 95% confidence (see appendix IV), consideration of the gradients of the upper, linear portions of the graphs, (the portion for which K'_b is greater than $20 \times 10^{-6} \text{ ohm}^{-1} \text{ cm}^{-1}$) shows a ratio of 1 : 3.3 from maximum to minimum gradient. In calculation of the mean value of the gradient that of SIC8/H must be excluded because its limits of variation are so large that a significant value for its gradient cannot be determined. If SIC8/CU is excluded the mean gradient is 1.79 mv^{-1} and the maximum variation from this mean is given by

$$1.79 \pm (1.79 - 1.11)$$

$$= 1.79 \pm 0.68$$

which is a variation of $\pm 36.8\%$. This is greater than the limits of error as calculated in appendix VI. If SIC8/CU is included the variation from the mean is

$$1.66 \pm (1.66 - 9.73)$$

6.3 - 2 With the = 1.66 ± 0.93 SIC8/CU the SIC8 series which is a variation of $\pm 56\%$

6.2 - 6 The order of decrease in gradient for the series from SIC5 to SIC8 for solutions of CuSO_4 and H_2SO_4 as individual salt is:

SIC6/CUB	SIC7/CU
SIC6/CUC	SIC8/CUB
SIC5/CU	SIC8/CU
SIC6/CU	
SIC6/H	

These results, which follow no obvious pattern, suggest that the change of magnitude of the zeta potential

with electrolyte concentration depends upon the specific bulk conductance, K'_b , of the solution and not upon the specific electrolyte which is present. They also suggest that the pretreatment received by the diaphragm material before use does not affect subsequent streaming potential measurements.

6.3 Interpretation of the results of SIC5 for combinations of copper sulphate and sulphuric acid, for copper sulphate and for sulphuric acid.

The experimental results were plotted on log/linear paper fig. 6.6.

With the exception of SIC5/ONE HALF HCU it was possible to draw straight line log/linear graphs through the experimental points and within the limits of 95% confidence for each determination. These results are shown in graph fig 6.6.

6.3 - 1 Compared with SIC6/CU, SIC6/CUB, SIC6/CUC and SIC6/H graph SIC5/CU was of lesser gradient but it had a similar gradient to SIC7/CU, SIC8/CU and SIC8/H.

6.3 - 2 With the exception of SIC5/CU the SIC5 series line with the smallest gradient was SIC5/ONE EIG HCU.

6.3 - 3 The order of decrease of gradient for SIC5 is:

- QTR ONE HCU
- ONE ONE HCU
- HALF ONE HCU
- EIG ONE HCU
- ONE QTR HCU
- H
- ONE EIG HCU
- CU

This order does not appear to follow any simple pattern

47

with respect to the relative proportions of H^+ and Cu^{++} present in the solution.

N.B. SIC5/ONE HALF HCU is a concave curve tending towards the vertical with increase in K'_b .

6.3 - 4 Consideration of the gradients of the graphs show that, excluding SIC5/CU, the ratio of the steepest to shallowest gradient is 1 : 2.32. The mean value of the gradients, excluding SIC5/CU and SIC5/H is 1.91 mv^{-1} . The variation from the mean is $1.91 \pm (2.32 - 1.91)$
 $= 1.91 \pm 0.41$

which is a variation of 21.4%. This compares closely to the limits of error as calculated in appendix VI.

6.3 - 5 These results for SIC5 would support the suggestion made in 6.2 - 6 that the change in magnitude of the zeta potential with electrolyte concentration depends upon the specific bulk conductance of the solution rather than on the specific ions present.

6.4 Interpretation of the results of series SIC9 for combinations of nickel and potassium sulphates, for nickel sulphate and for potassium sulphate.

For this series it was not possible to draw straight line log/linear graphs through the experimental points and within the limits of 95% confidence. The results are shown in fig. 6.7. The lines are superficially the same shape as those for copper sulphate and sulphuric acid on silicon carbide and they all show a more marked zeta potential maximum. No explanation can be offered regarding the reason for this maximum which falls between the K'_b values of $9 \text{ to } 23 \text{ ohm}^{-1} \text{ cm}^{-1} \times 10^{-6}$, giving a mid point of

$16 \text{ ohm}^{-1} \text{ cm}^{-1} \times 10^{-6}$. This value is higher than the mid point value for SIC5 to SIC8 as shown in figs. 6.4 and 6.5

Although there was a certain amount of pattern in the zeta potential maxima this was insufficient to draw conclusions from.

These curves show a general downwards drift of zeta potential with time as was noticed in SIC5 to SIC8, figs. 6.4 and 6.5 (see 6.2). It is not possible to determine the actual gradients of the upper portions of the curves, i.e. the portion for which K'_b is greater than the zeta potential maximum, as they are not sufficiently near to linearity. Although no pattern can be distinguished in the order of apparent decrease of gradient of the upper portion of these curves it is possible that the curves may have become linear at higher electrolyte concentrations in the same way as did those for copper sulphate and sulphuric acid (see figs. 6.4 and 6.5). This could not be checked with the existing apparatus as it is unfortunately impossible to make accurate measurements of the streaming potentials generated when using concentrated solutions.

6.5 Results of zeta potential measurements on silicon carbide using potassium chloride solutions, series SIC5 and SIC9.

For both SIC5 and SIC9 the graph of K'_b vs zeta potential showed a zeta potential maximum but also in each case a straight line could be drawn through the points above this maximum: fig. 6.8. The straight line portions of the graphs were parallel within the limits of 95% confidence.

6.6 Results of the investigation on chromium diboride using copper sulphate and sulphuric acid, series CRB2.

With each electrolyte the zeta potential on chromium diboride was initially just about zero and became increasingly positive with increasing K'_b . With sulphuric acid solutions the zeta potential increased linearly with K'_b and with copper sulphate solutions a slightly convex curve was obtained: fig 6.9.

6.7 Change in zeta potential with increase in ionic strength of the solution.

As the ionic concentration of a solution in contact with silicon carbide or chromium diboride is increased the value of the zeta potential becomes more positive. If graphs in figs 6.4, 6.5 and 6.6 are considered and if the straight lines were extrapolated as for an increase in K'_b they would pass through the zero point of zeta potential. In the case of series SIC5, fig 6.6, the value of K'_b for zeta equal to zero is in the order of $1000 \times 10^{-6} \text{ ohm}^{-1} \text{ cm}^{-1}$; this corresponds to a salt or acid concentration of much less than 0.01M so that when in contact with a solution of the concentration normally used for copper plating (approximately 1M CuSO_4 and 0.5M H_2SO_4 the zeta potential may be expected to have a positive sign. *) Elton Cairns & Maslin

N.B. An estimate of the zeta potential of a silicon carbide particle in a copper plating solution was obtained by extrapolating fig 6.6 to the value of bulk conductance in this plating solution. The figure obtained from this rather long extrapolation was about + 20 mv.

Any electrophoretic transport will be towards the cathode for both silicon carbide and chromium boride. Transport for chromium boride in a given potential gradient would be higher as for a given ionic strength of solution it has a higher zeta potential, (see figs 6.4, 6.5 and 6.9).

These conclusions regarding the sign of the zeta potential on silicon carbide are supported by the results of Fairbrother and Mastin,⁶¹ Perrin⁶⁶ and Elton⁶⁷ who showed that the zeta potential on silicon carbide became more positive with increasing concentration of salt and of acid.

Results of Perrin: Solution and concentration. Zeta Potential, mV

HCl	0.02N	+ 10
HCl	0.0008N	0
KBr	0.1M	- 14
HCl	0.0002N	- 15
La(NO ₃) ₃	0.0002M	- 18
Ba(NO ₃) ₂	0.002M	- 26
Water		- 60
KOH	0.0002N	- 60
KOH	0.002N	-105

Results of Elton and of Fairbrother & Mastin:

KCl solution on SiC, Concentration (M)	Zeta Potential, Elton (sedimentation)	Zeta potential, Fairbrother & Mastin (Electroosmosis)
1×10^{-5}	265	-
2×10^{-5}	255	73
1×10^{-4}	223	66
1×10^{-3}	172	50

Elton's results are higher than those of Fairbrother and Mastin but the ratio is almost constant at about 3.4 : 1.

Our results are lower by about 3:1 than those of Fairbrother and Mastin, falling in the range -4 to -36mV.

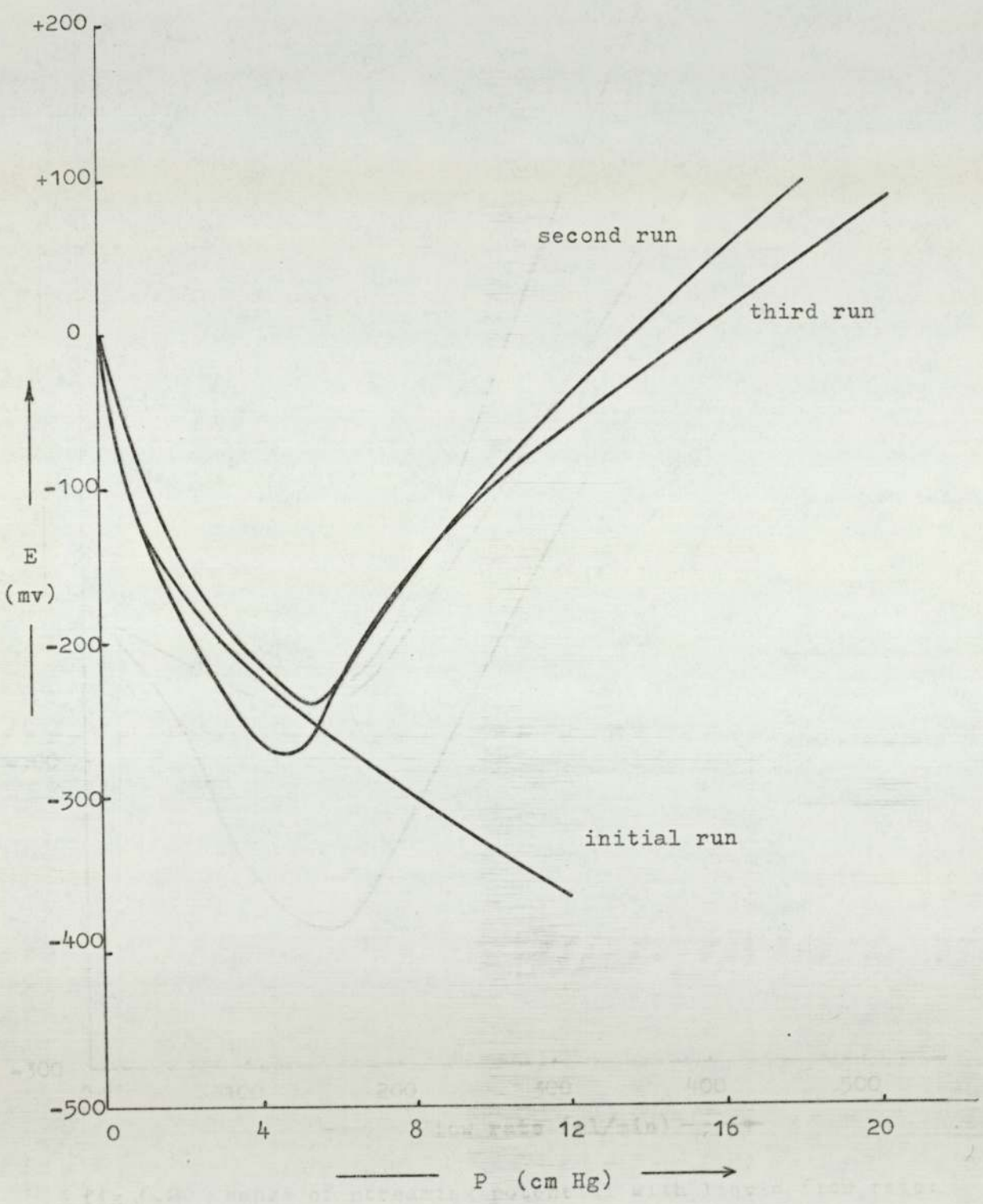


fig 6.1 Change of streaming potential with hydrostatic pressure: alumina/water.

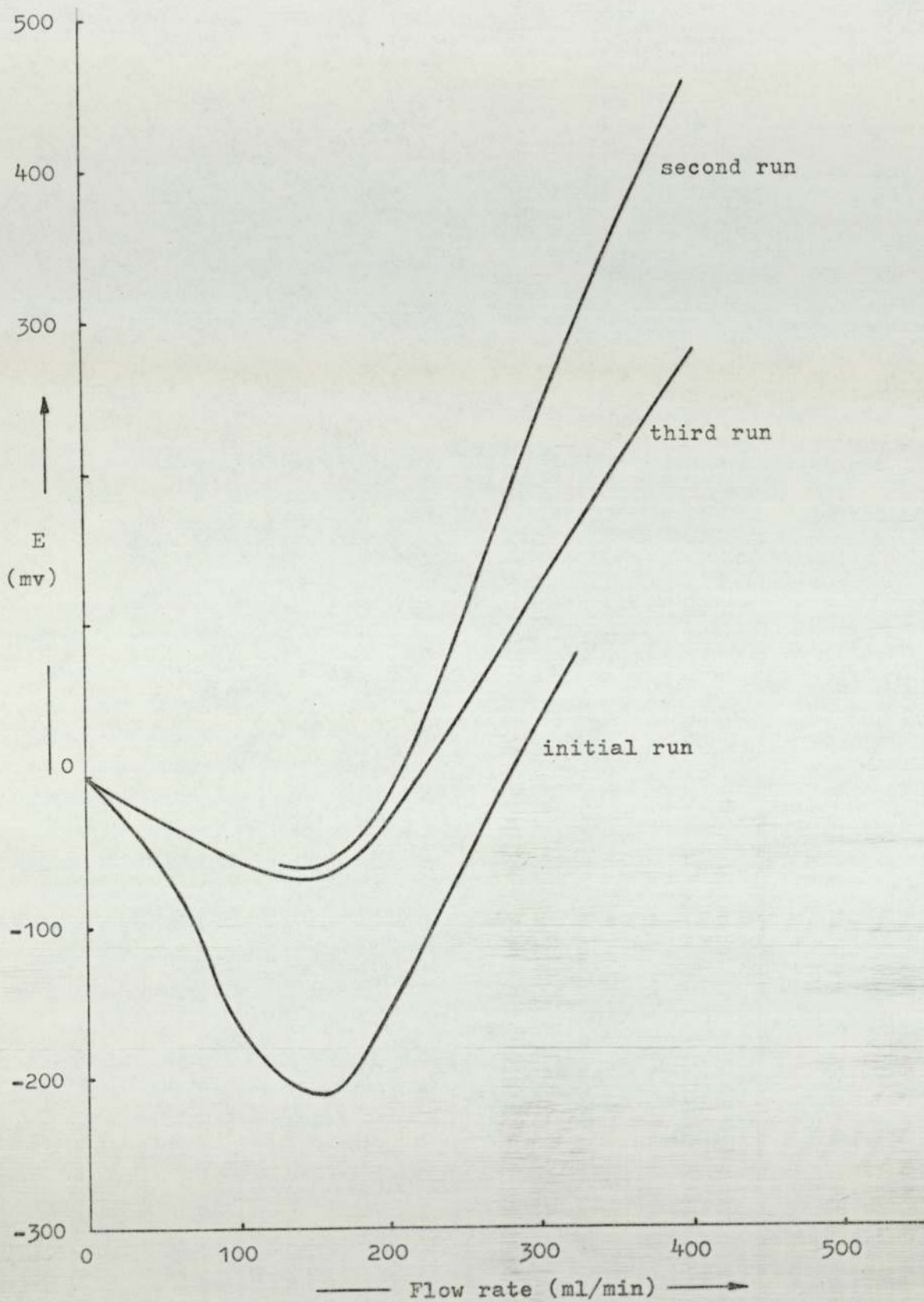


fig 6.2 Change of streaming potential with liquid flow rate: alumina/water.

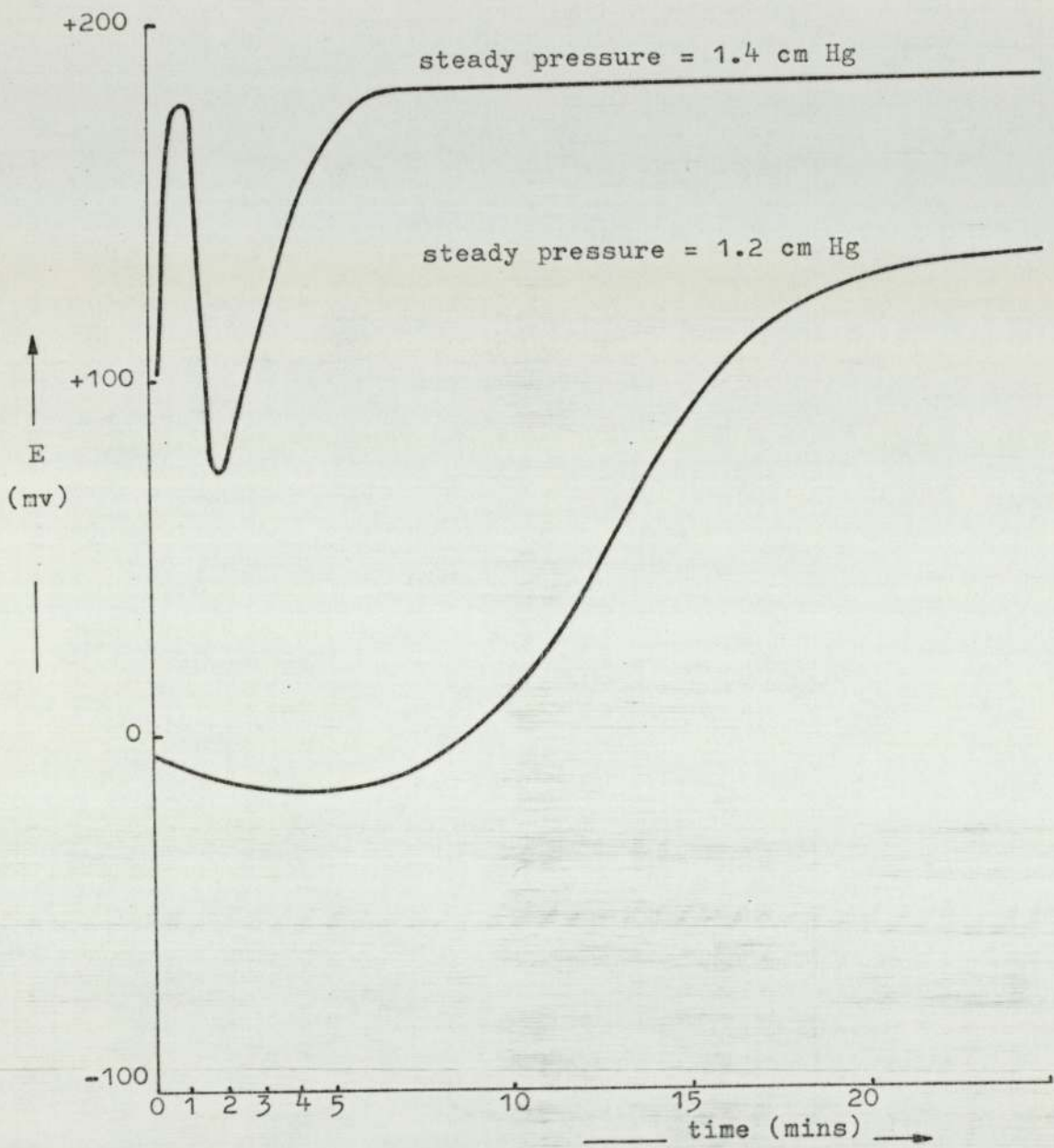


Fig 6.3 Change of streaming potential with time under constant pressure: alumina/water.

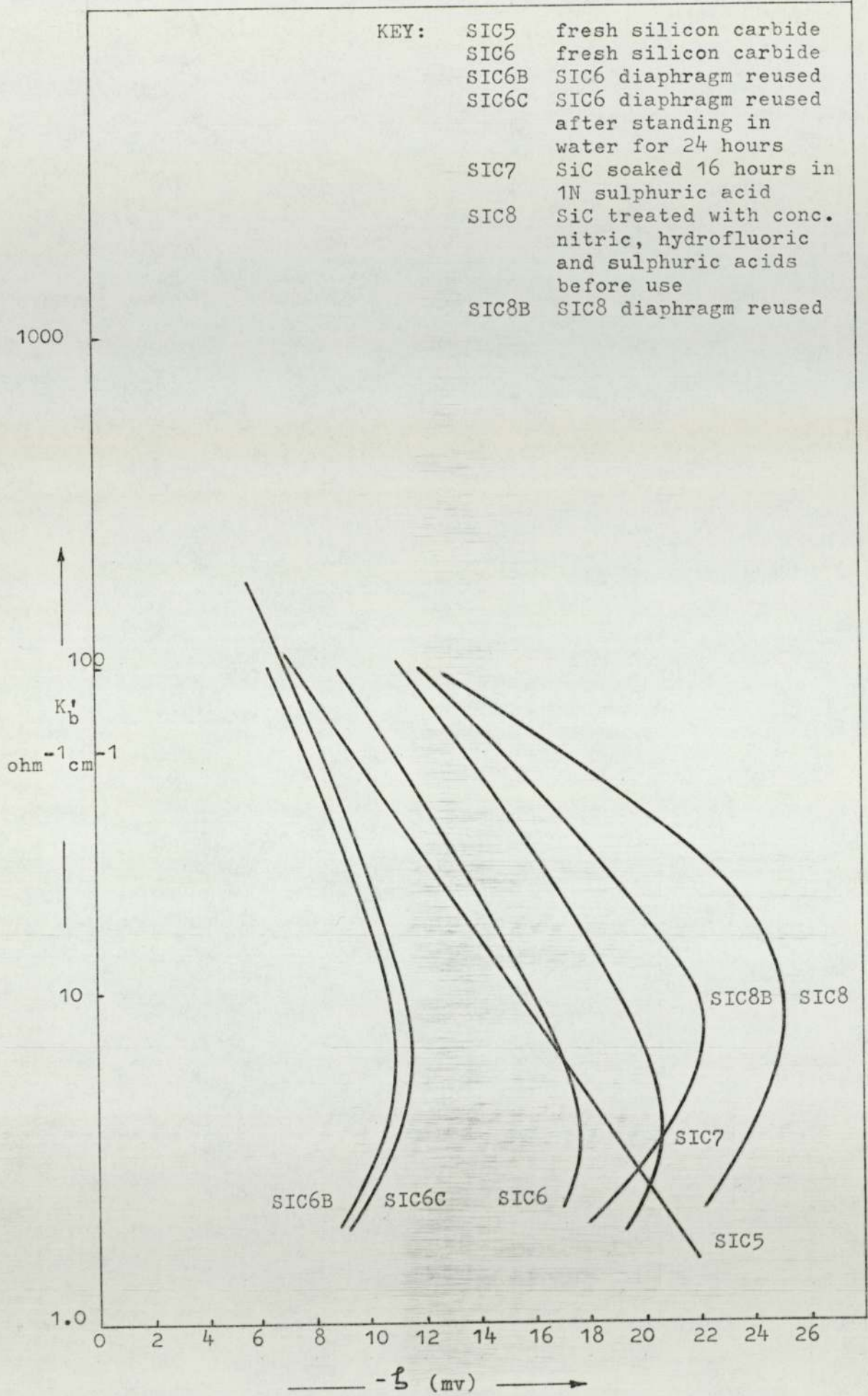


fig 6.4 Change of zeta potential with K_b' : silicon carbide with copper sulphate.

KEY: SIC6H SIC6 with sulphuric acid
 SIC8H SIC8 with sulphuric acid

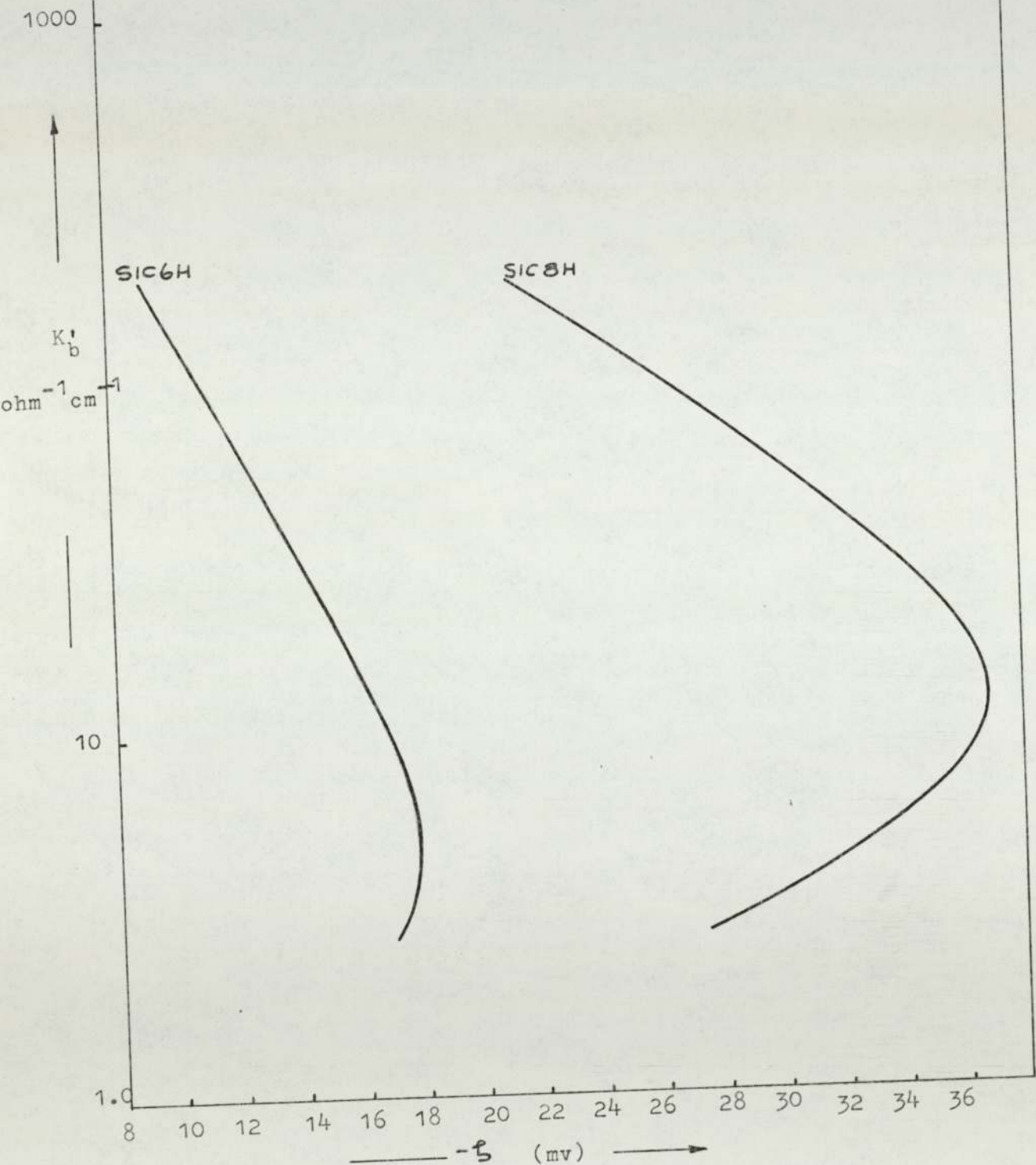


fig 6.5 Change of zeta potential with K'_b : silicon carbide with sulphuric acid.

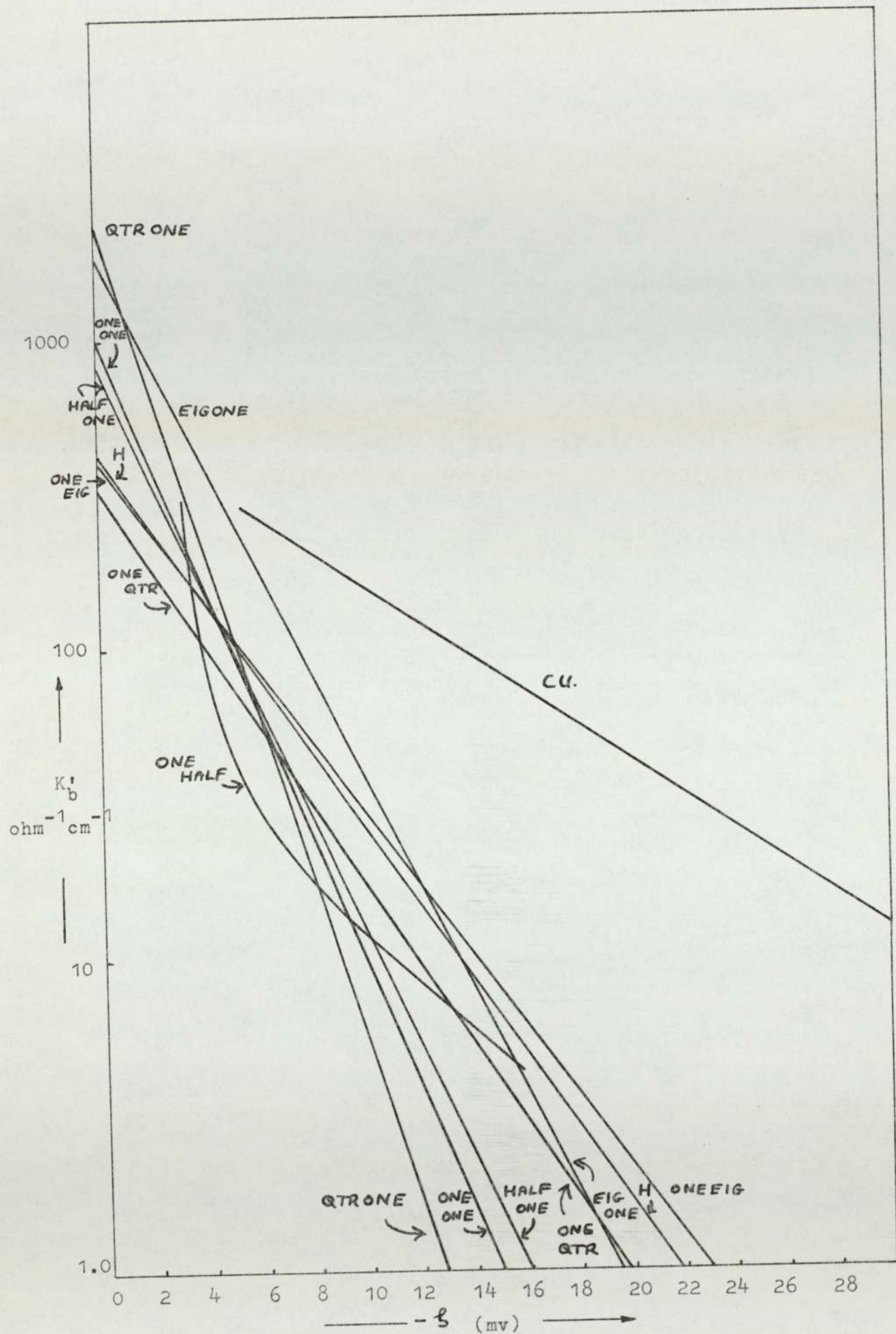


fig 6.6 Series SIC5: change of zeta potential with K'_b for silicon carbide with CuSO_4 , H_2SO_4 and $\text{CuSO}_4/\text{H}_2\text{SO}_4$ mixtures.

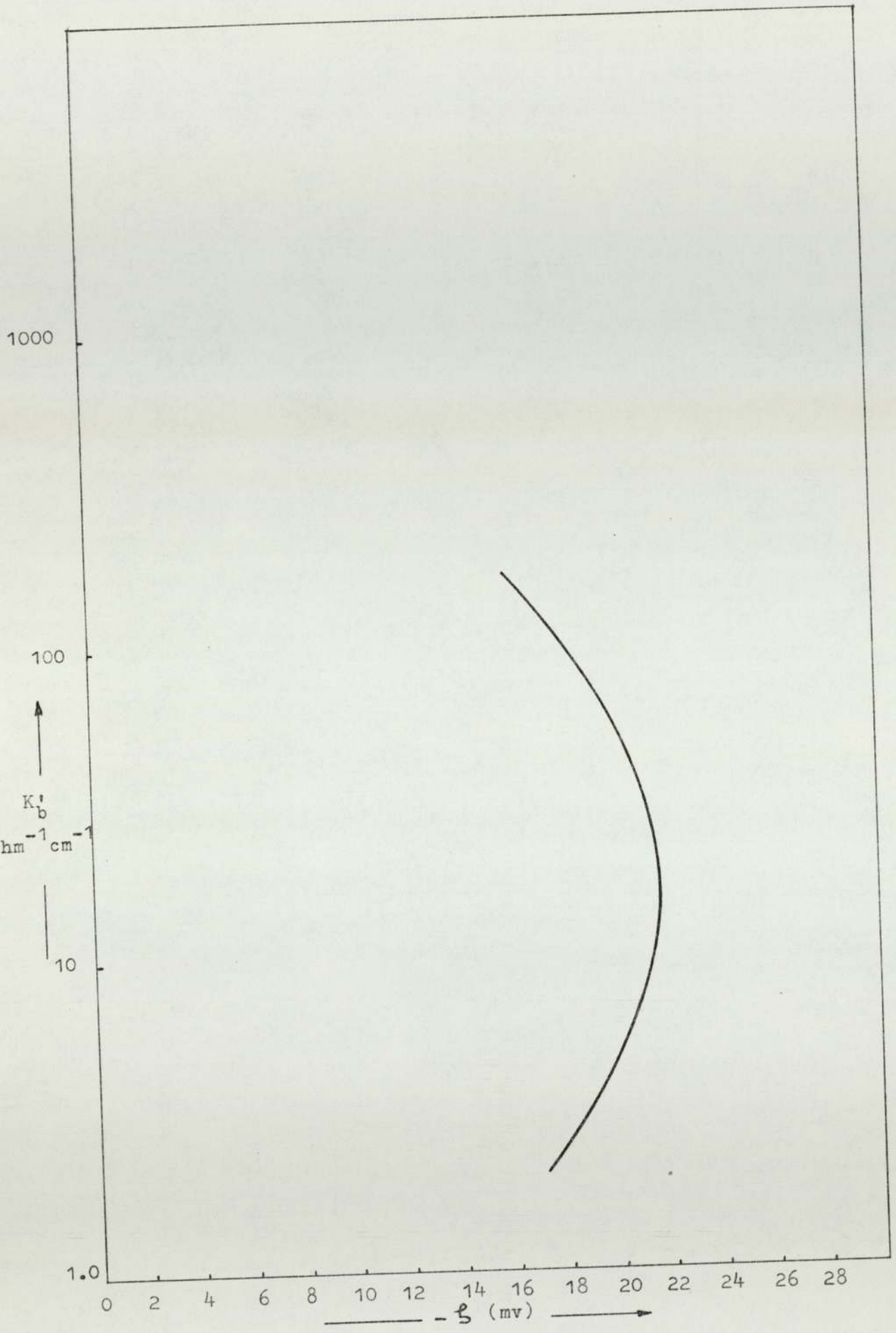


fig 6.7 Series SIC9: change of zeta potential with K'_b for silicon carbide with $NiSO_4$, K_2SO_4 , $NiSO_4/K_2SO_4$ mixtures. Graph shown is for SIC9/ONEHALF NIK as being typical of this series.

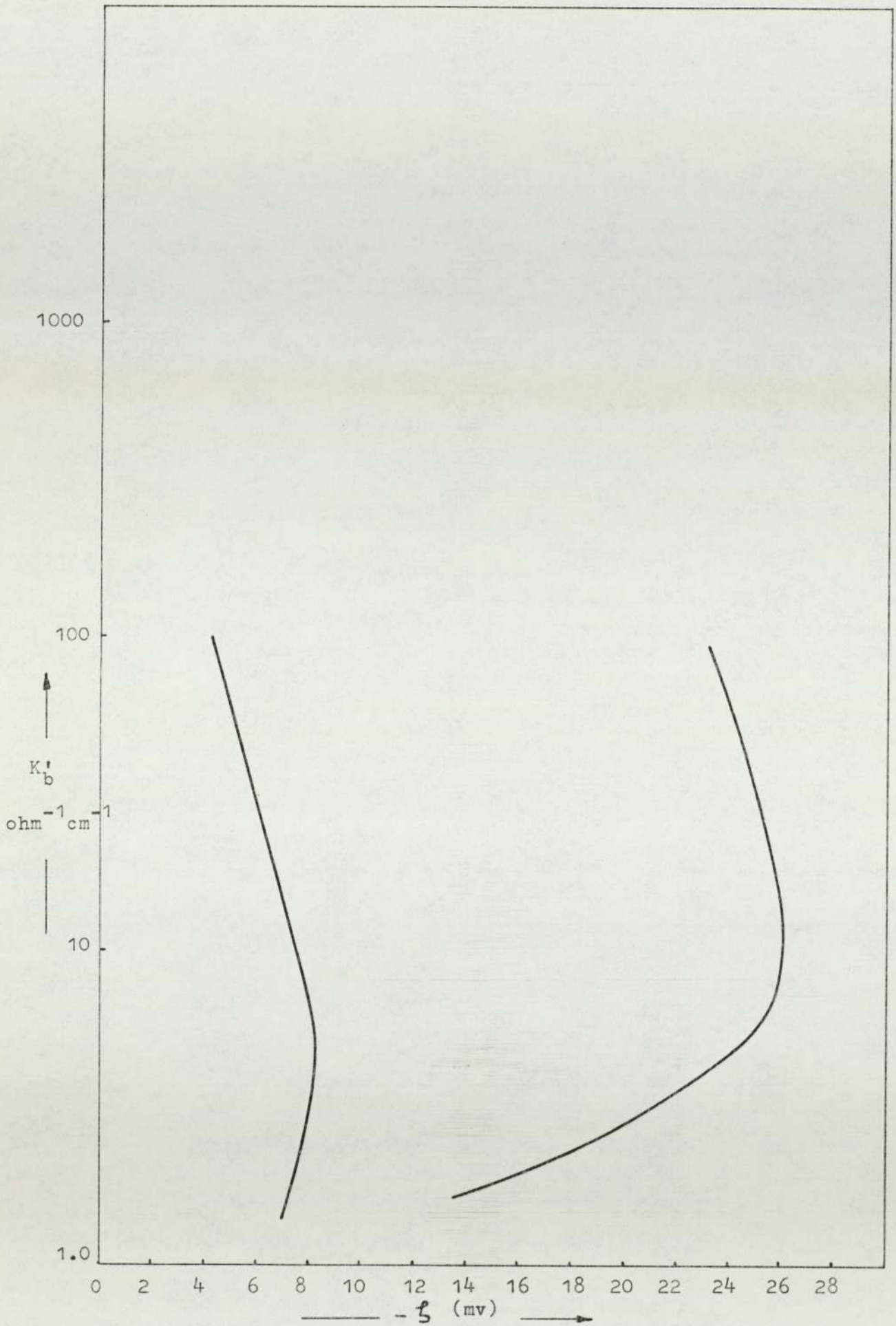


fig 6.8 Change of zeta potential with K'_b : silicon carbide with potassium chloride.

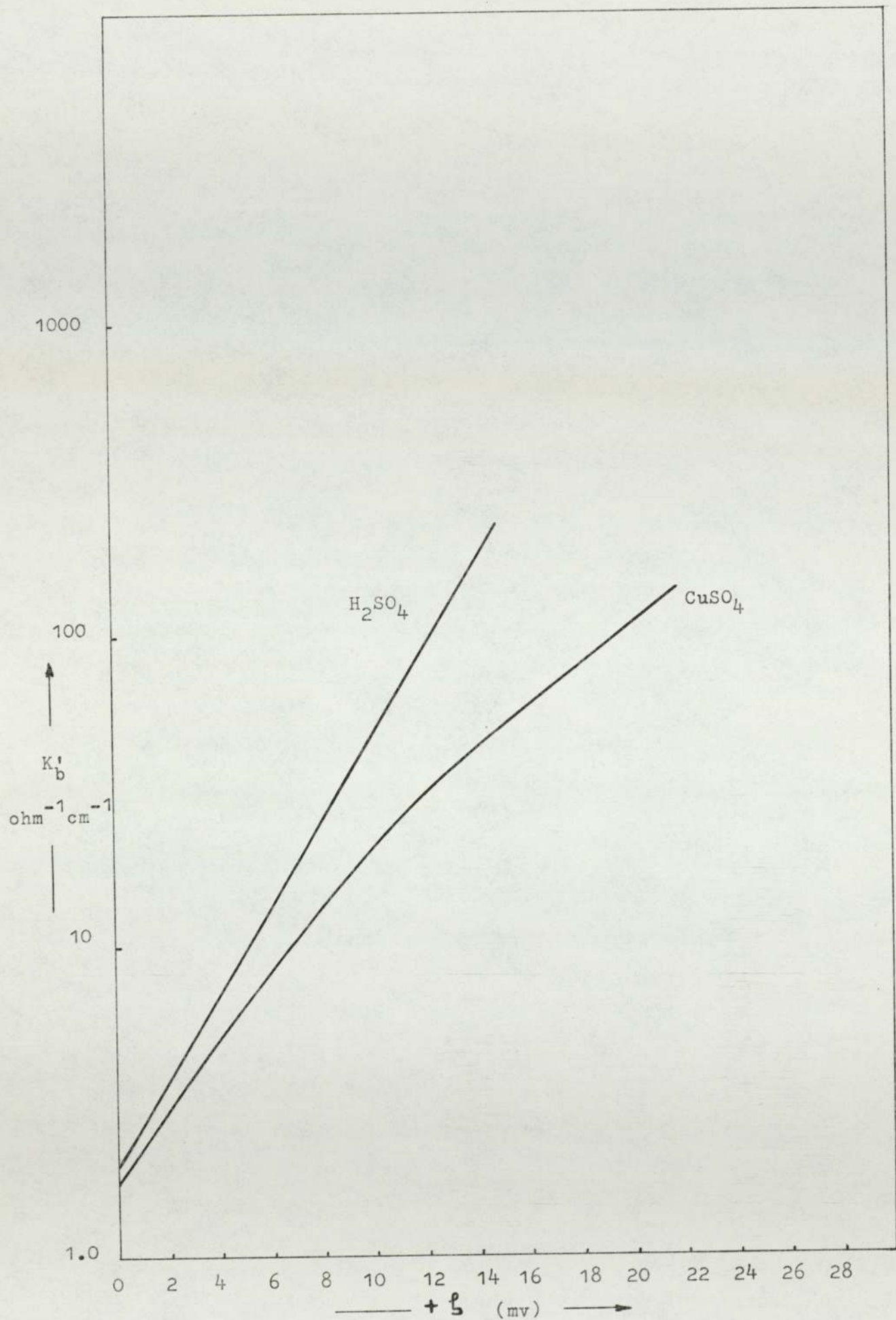


fig 6.9 System CRB2: change of zeta potential with K'_b , chromium diboride with copper sulphate and with sulphuric acid.

Chapter 7. PREPARATION AND EXAMINATION OF CERMET

ELECTRODEPOSITS.

7.1 Preparation of deposits

Composite copper/silicon carbide and copper/chromium diboride materials were prepared under conditions typical of those used by Williams and Martin.²¹ The bath loading of ceramic powder was 100g per litre of solution and was dispersed through the solution by prolonged stirring with a mechanical stirrer. The silicon carbide used was of mean particle size 4.5 microns and the chromium diboride of mean particle size 11 microns. The electrolyte was a conventional copper sulphate - sulphuric acid copper plating bath of composition:

copper sulphate pentahydrate	250g
sulphuric acid, concentrated	50g
water	to 1 litre.

This solution was used at room temperature and at a cathode current density of 50 mA cm^{-2} onto brass strips of size $2.5 \times 5 \times 0.2 \text{ cm}$. The corners of these strips were rounded by filing to reduce treeing at these points. Plating times were of up to 30 hours, giving deposits of thickness up to 0.15 cm.

Prior to electroplating each brass strip was degreased in trichloroethylene vapour, abraded with dry 280 grade emery paper, immersed for 15 seconds in 25% nitric acid and finally washed in distilled water. Before drying could take place it was suspended in the plating bath; electrical contact was made after immersion.

Plating was carried out in a 2 litre glass tank of dimensions $20 \times 12.5 \times 12.5 \text{ cm}$. A copper anode was mounted at one end of the tank and the brass strip cathode was

suspended, with three quarters of its length immersed in the electrolyte, at about 5 cm from the other end and with its face parallel to that of the anode. The ceramic was maintained in suspension by a mechanical stirrer placed centrally in the tank. Just sufficient agitation was used to maintain the ceramic in suspension.

The D.C. supply was full-wave rectified A.C. produced by transforming and rectifying mains A.C. Plating potential was controlled by means of a rheostat; no voltage stabiliser was used. Small variations of cathode current density were observed during plating but these were considered insignificant.

7.2 Electrophoretic transport of a charged particle in an electrolyte solution.

A charged particle suspended in a liquid can be transported, under the influence of an applied potential, by electrophoresis. If the following are taken as specimen conditions the rate of electrophoretic transport of such a charged particle can be calculated.

Specimen conditions:

Zeta potential on the particle = +20 mV (see 6.7.)

Potential gradient = 0.25 V cm⁻¹

For the expression $v = \frac{DE\xi}{4\pi\eta_0}$ v is the electrophoretic velocity of the particle in cm sec⁻¹, D is the dielectric coefficient and η_0 the coefficient of viscosity of the solvent (see A2.2 - 1.) in poises.

$$\text{At } 25^\circ\text{C} \quad v = \frac{78.3 \times 0.25 \times 20 \times 10^{-3}}{4 \times 3.142 \times 8.949 \times 300 \times 300 \times 10^{-3}}$$

$$v = \underline{5 \times 10^{-5} \text{ cm sec}^{-1}}$$

Thus under plating conditions a particle with a zeta potential of +20 mV would be moved only 5×10^{-5} cms per second by electrophoresis in the bulk of the solution. This is quite negligible when compared with mechanical or hydrodynamic transport.

Within the diffuse portion of the double layer the effects of dielectric saturation or specific solvent orientation are not very important. However appreciable saturation can arise in the higher field region near to the electrode surface.⁷⁴ Also, within the double layer the potential gradient is much greater than that in the bulk of the solution as shown in fig 4.4. If within the fixed portion of the double layer the potential gradient rose to 100 times its bulk value and the dielectric coefficient fell to 0.1 of its bulk value the velocity of electrophoretic transport would rise to 5×10^{-4} cm sec.⁻⁸ cm (see A1.1) and the particle would pass through this double layer in 3×10^{-5} seconds. This suggests that electrophoretic transport through the double layer may be the mechanism by which a particle is transferred to the cathode surface once it has been hydrodynamically transported to the surface of the fixed portion of the double layer. Figs. 7.1 to 7.3 illustrate the difference in behaviour of charged particles of equal size being hydrodynamically transported parallel to the surface of a cathode. Fig. 7.1 shows the path that would be taken in the absence of any field at the cathode i.e. in the absence of electrophoresis, fig. 7.2 shows the path taken by particles carrying a small positive charge when they come into the field of the cathode and fig. 7.3 shows the path taken by particles carrying a relatively large positive

charge when they come into the cathode field.

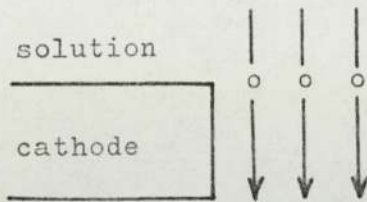


fig 7.1 Charged particle passing a cathode in the absence of a cathode field.

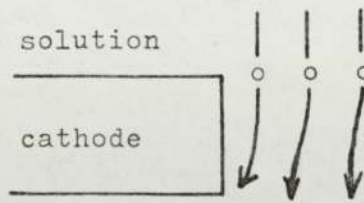


fig 7.2 Particle of small positive charge passing through the cathode field.

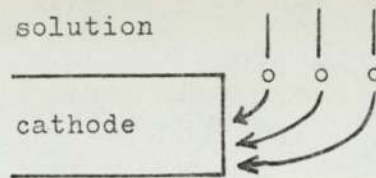


fig 7.3 Particle of large positive charge passing through the cathode field.

A particle having a high positive charge is most likely to be deposited by electrophoresis as it will be transported towards the cathode most rapidly. The above calculations show that provided the particles are transported hydrodynamically to the vicinity of the cathode surface electrophoresis should play a significant role in their subsequent deposition.

of 5.481 coulombs is $\frac{5.418}{50 \times 10^{-3}}$ seconds

2 minutes

(assuming 100% cathode efficiency)

N.B. The time to key a particle could be less than 2 minutes if the particle was in a trough in the surface of the electrodeposit (see 8.1 - 1.) as shown in fig. 7.4 (a) and (b).

7.3 Time required to mechanically key a particle into an electroplated coating.

A particle may be considered to be keyed in position when metal is deposited around it to a thickness greater than half of its diameter (assuming a spherical particle). For a 4 micron particle 2 microns of copper are required for keying; the particle must remain stationary and in contact with the cathode surface for the time required to deposit this thickness of copper.

Consider an electrodeposit of area 1 cm^2 and thickness $2 \times 10^{-4} \text{ cm}$:

$$\text{volume of this deposit} = 2 \times 10^{-4} \text{ cm}^3.$$

$$\begin{aligned} \text{mass of this deposit} &= 8.92 \times 2 \times 10^{-4} \text{ g} \\ &= \underline{1.784 \times 10^{-3} \text{ g.}} \end{aligned}$$

Time required to deposit this mass of copper:

31.77 g of copper will be deposited by 96500 coulombs of charge hence $1.784 \times 10^{-3} \text{ g}$ will be deposited by

$$\begin{aligned} &\frac{96500 \times 1.784 \times 10^{-3}}{31.77} \\ &= \underline{5.481 \text{ coulombs.}} \end{aligned}$$

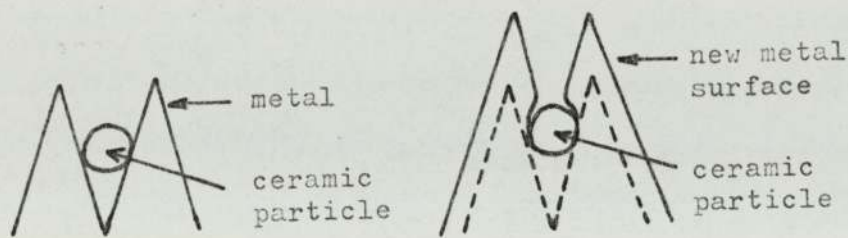
Under plating conditions the cathode current density is 50 mA cm^{-2} , hence the time required for the passage of 5.481 coulombs is

$$\frac{5.418}{50 \times 10^{-3}} \text{ seconds}$$

$$\underline{2 \text{ minutes}}$$

(assuming 100% cathode efficiency)

N.B. The time to key a particle could be less than 2 minutes if the particle was in a trough in the surface of the electrodeposit (see 8.1 - 1.) as shown in fig. 7.4 (a) and (b).



(a) ceramic particle in a trough
 (b) particle keyed into place: dotted lines show original surface.

Fig 7.4 Keying of a particle on a rough cathode surface.

7.4 Examination of cermet electrodeposits.

Examination of the deposits prior to polishing showed that for a deposit thicker than about 0.02 cm there was considerable surface roughness, giving a surface contour having considerable depth between the high and low points. This was least in the centre of the face of the specimen and increased towards the edges, ending in some treeing. This roughness increased with deposit thickness and was greater, for a given deposit thickness, than the roughness of a deposit of copper without inclusions. The rough deposit trapped a considerable amount of ceramic powder which could be clearly seen in the crevices and hollows of the surface with the aid of a hand lens. It was most noticeable in the treed edge build-up.

Sections parallel to and transverse to the specimen surface were prepared and polished for microexamination. The polishing sequence was wet rubbing on graded wet-or-dry papers down to 600 grade followed by final polishing

with quarter micron size diamond paste on a revolving pad.

Polished specimens were examined and photographed using a metallurgical optical microscope (Reichert "Me F" Universal Camera Microscope) and a scanning electron microscope (Stereoscan Mk II, Cambridge Instrument Company). Optical microscopy, with magnifications of between 50 and 200 diameters, was used to determine the distribution of the ceramic particles through the deposit and scanning electron microscopy, with magnifications of up to 54000 diameters, to examine the metal-ceramic interface. The aim in examining the interface was to determine whether (a) there was any space between the matrix metal and the ceramic or (b) if there was an intermediate solid phase separating them (see 1.5 - 2). Any such solid phase would probably have been formed either by chemical reaction between the metal and the ceramic or by inclusion of salts from the plating bath due to the use of incorrect operating conditions.

To see if the presence of ceramic inclusions causes significant distortion in the structure of electrodeposited copper a number of transverse sections were etched in ammonium persulphate solution (10% solution for 4 minutes at room temperature) to expose the structure of the copper deposit. These sections were then examined with the optical microscope.

N.B. The rather long etching time was necessary because the brass strip which was in contact with the copper deposit "galvanically" protected the copper from attack by the reagent.

Chapter 8. RESULTS AND DISCUSSION OF ELECTRODEPOSITION
EXPERIMENTS.

8.1 Distribution of ceramic through the metal matrix.

8.1 - 1 Silicon carbide in copper.

The lowest proportion of ceramic particles was in the centre of the strip specimen; the proportion increased towards its edges. The surface roughness of the specimen was greatest at its edges (see 7.4) and the highest inclusion density was therefore in the roughest portion: in fig. 8.1 an uneven pattern can be seen; this corresponds to an increased inclusion density in the parts of the deposit which correspond to the troughs in the surface of the electroplate. This suggested that the ceramic had tended to collect in the troughs, possibly because of the shielding effect of the crests, remaining on the metal surface until keyed by metal. This is shown diagrammatically in fig 8.2.

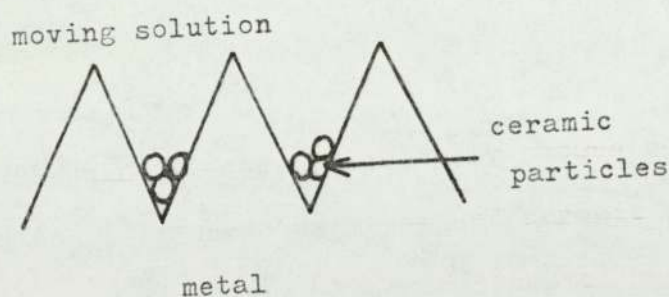


Fig. 8.2 Diagrammatic representation of the surface contour of a deposit showing the shielding of particles in a trough.

The increase in particle density at the edge of the specimen and the high proportion of inclusions in the edge build-up are shown in figs. 8.3 and 8.4 respectively. The porous structure of the edge build-up can be clearly seen.

The density and distribution of ceramic was similar in the deposits on the sides facing and remote from the anode, as can be seen in figs. 8.5 and 8.6. As powder having a small size range was being used (maximum limits 1-10 microns with most in a much smaller range) the particle size distribution was, as expected, fairly even. N.B. In fig. 8.5 the top surface of the specimen is flat because it was polished (for examination) parallel to its surface prior to being sectioned.

8.1 - 2 Chromium diboride in copper.

The results were similar to those obtained for silicon carbide, a much higher proportion of inclusions being found in the rough edge build-up than in the centre of the strip specimen. An increase in the inclusion density with increasing roughness of the deposit can be clearly seen in figs. 8.7, 8.8 and 8.9. Figs. 8.10 and 8.11 show the distribution of inclusions transverse to the surface. The particle size distribution was again fairly even.

8.2 The metal-ceramic boundary.

Scanning electron microscopy showed no intermediate solid phase between the metal and ceramic and no large space separating them. The presence of a third phase was not expected as any chemical reaction between metal and ceramic would need to have taken place at room temperature. The ceramic particles appear to be simply mechanically imbedded in the matrix metal, as shown in fig. 8.12.

N.B. Examination, by ^{the Author} Δ , of nickel/vanadium diboride material produced by Isserlis²⁵ under conditions similar to those used in this work gave the same results.

8.3 The effect of ceramic inclusions on the structure of the matrix metal.

The presence of the ceramic inclusions did not appear to affect the structure of the copper electrodeposit; the copper grains appear to have grown around the ceramic particles without becoming distorted. It did not appear that the inclusions had collected predominantly at any one particular part of the structure e.g. at grain boundaries. Transverse sections, etched in 10% ammonium persulphate, are shown in figs. 8.13 and 8.14. It was noticed that many of the ceramic inclusions had fallen out of the surface of the etched specimens, e.g. see fig. 8.13.

8.4 Summary of the results of cermet electrodeposition.

The results of the electrodeposition work have shown that it is not difficult to obtain solid inclusions in electrodeposited copper by empirical methods. Although no direct evidence regarding the mechanism by which the particles are deposited on the cathode or how they are held in the matrix was obtained, there is strong evidence that mechanical entrapment of particles plays a significant part in the process of particle inclusion. The inclusion density was lowest in the centre of the specimen, increasing towards the edges (where the surface roughness was greatest) and being greatest in the edge build-up. An irregular distribution of inclusions parallel to the surface of the specimens appeared to correspond to the troughs in the rough surface of the deposit.

There is no general agreement between workers regarding the relationship between cathode current density and proportion of inclusions obtained in a deposit; the fact

that the current density is higher at the edges of the specimen was not considered to be the cause of the high inclusion density at these high current density areas.

No evidence of chemical bonding between the imbedded particles and the metal matrix was found; when a polished specimen was etched many solid particles fell out of the matrix suggesting that they had been simply mechanically held in position.

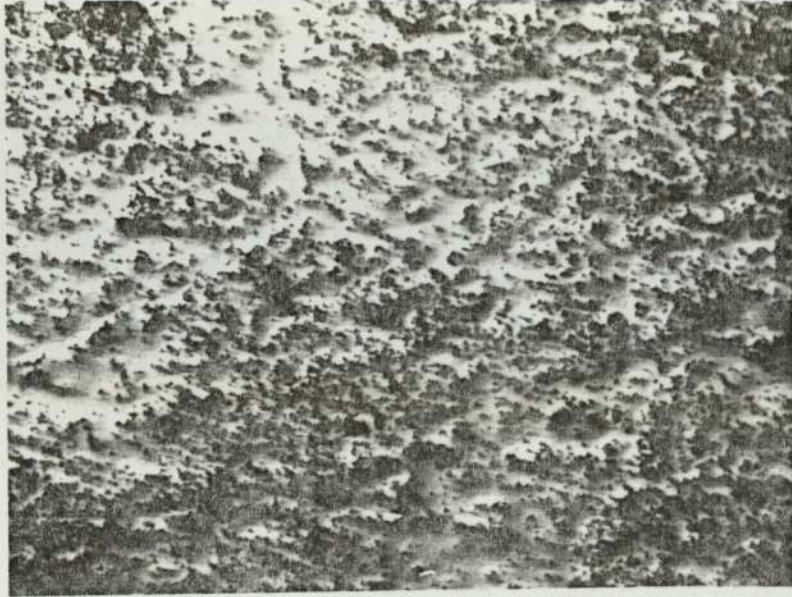


Fig 8.1 Uneven inclusion density corresponding to troughs in the surface of the electrodeposit. Silicon carbide in copper, parallel to surface. x 50 enlarged x3.



Fig 8.3 Increase in inclusion density at the edge of a specimen. silicon carbide in copper, parallel to surface. x 50 enlarged x 3.



Fig 8.4 High inclusion density in the edge build up:
the porous nature of this portion of the
deposit can be clearly seen.
silicon carbide in copper, parallel to surface.
x 50 enlarged x 4.

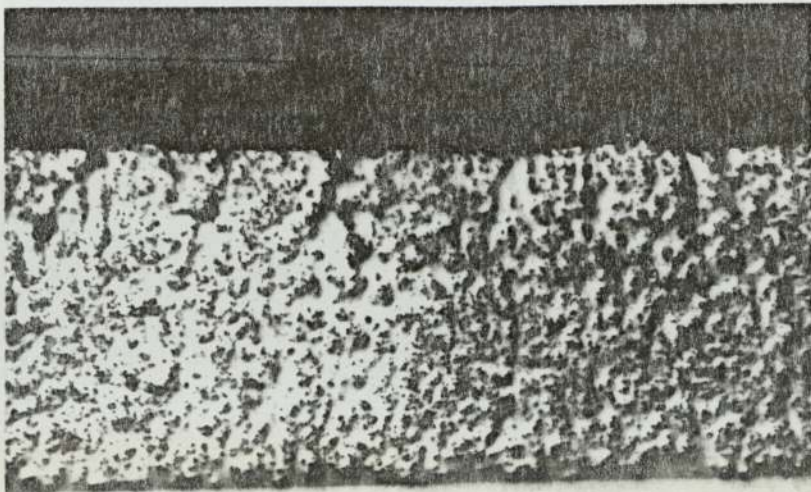


Fig 8.5 Inclusion distribution in an electrodeposit:
side of cathode facing the anode.
Silicon carbide in copper, transverse section.
x 50 enlarged x 3.

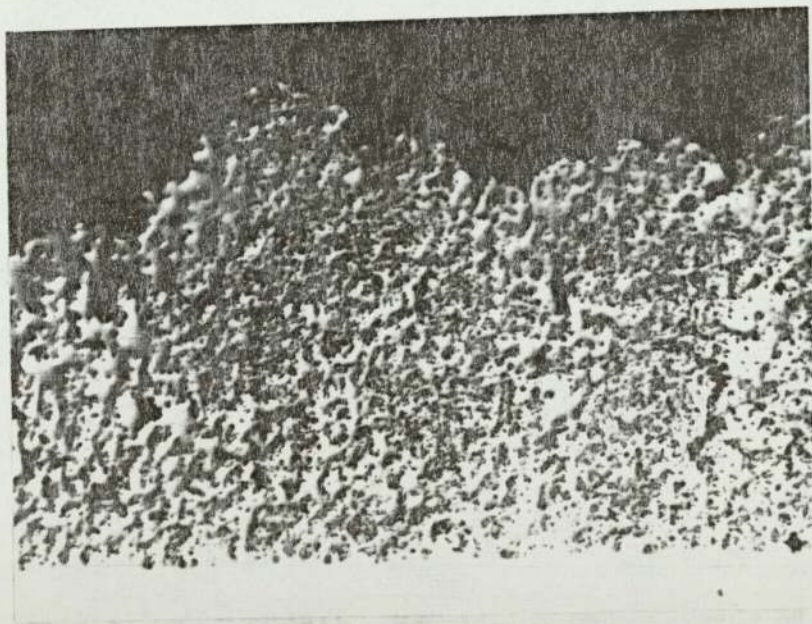


Fig 8.6 Inclusion distribution in an electrodeposit:
side of cathode remote from the anode, the
same specimen as in fig 8.5.
Silicon carbide in copper, transverse section.
x 50 enlarged x 3.



Fig 8.7 Uneven inclusion density corresponding to troughs in the surface of the electrodeposit. Chromium diboride in copper, parallel to surface. x 50 enlarged x 3.

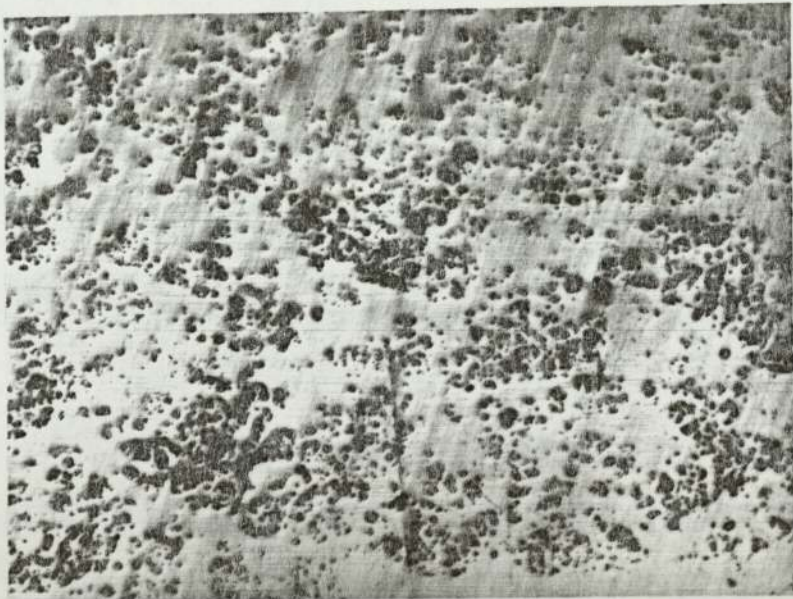


Fig 8.8 Increase in inclusion density, compared with 8.7, at the edge of a specimen: the uneven inclusion density is evident. Chromium diboride in copper, parallel to surface. x 50 enlarged x 3.

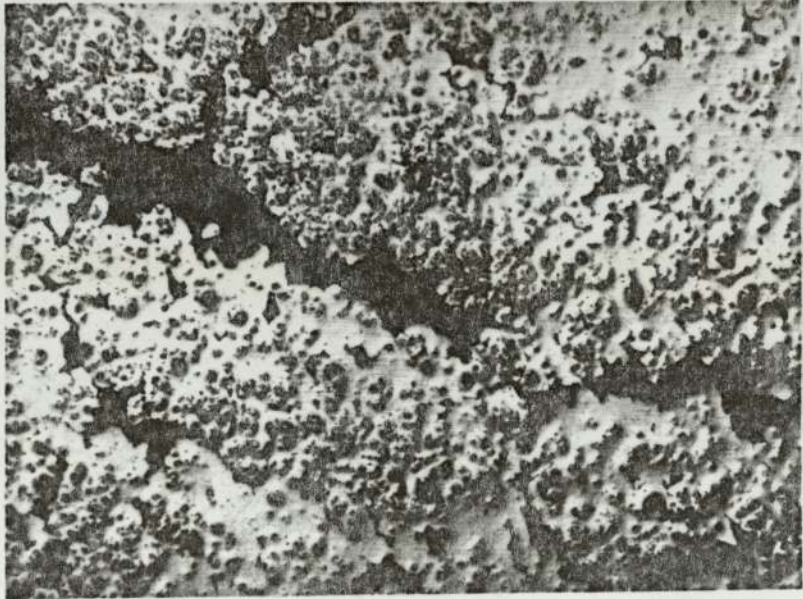


Fig 8.9 High inclusion density in the edge build-up:
the porous nature of the deposit can be clearly
seen.
Chromium diboride in copper, parallel to
surface.
x 50 enlarged x 3

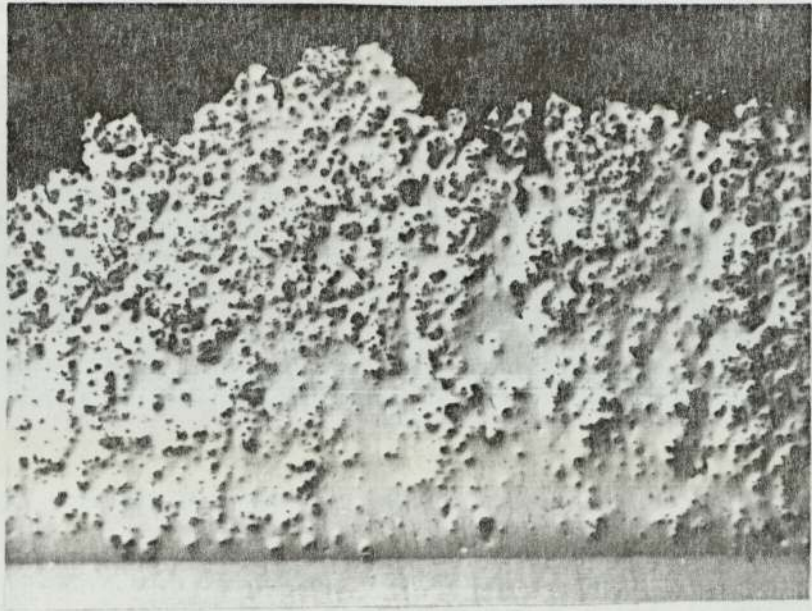


Fig 8.10 Distribution of inclusions on the side of the cathode facing the anode. Chromium diboride in copper, transverse section. x 50 enlarged x 3.

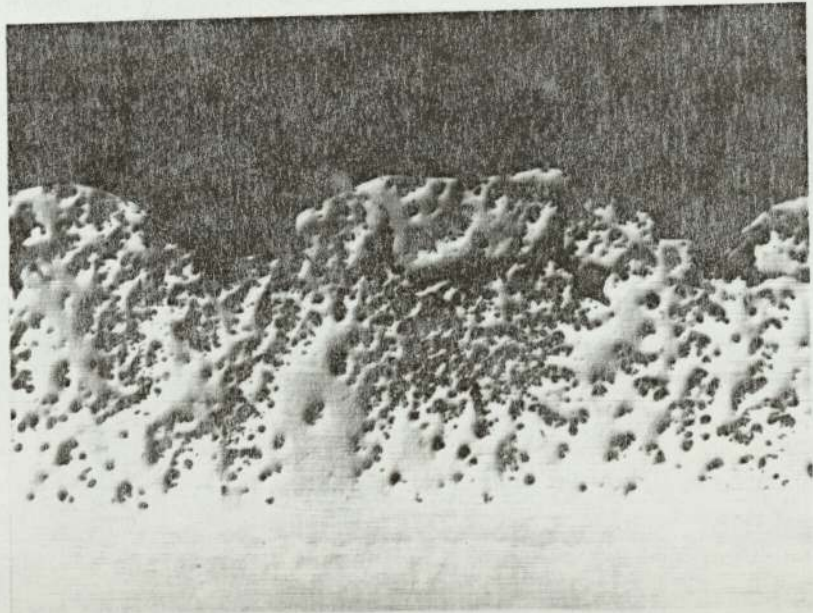


Fig 8.11 Distribution of inclusions on the side of the cathode remote from the anode: same specimen as in fig 8.10. Chromium diboride in copper, transverse section. x 50 enlarged x 3.

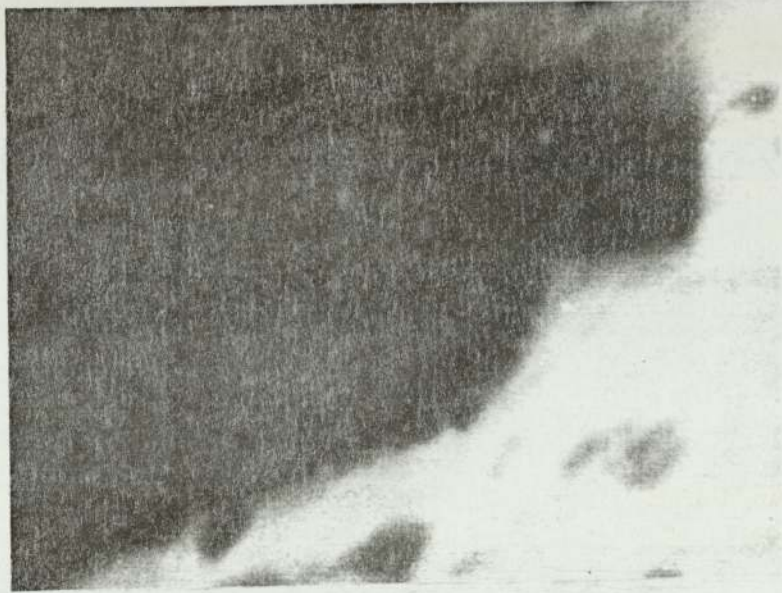


Fig 8.12 Ceramic particle embedded in a metal matrix.
Silicon carbide in copper.
Scanning electron micrograph, x 6000 enlarged
x 6.

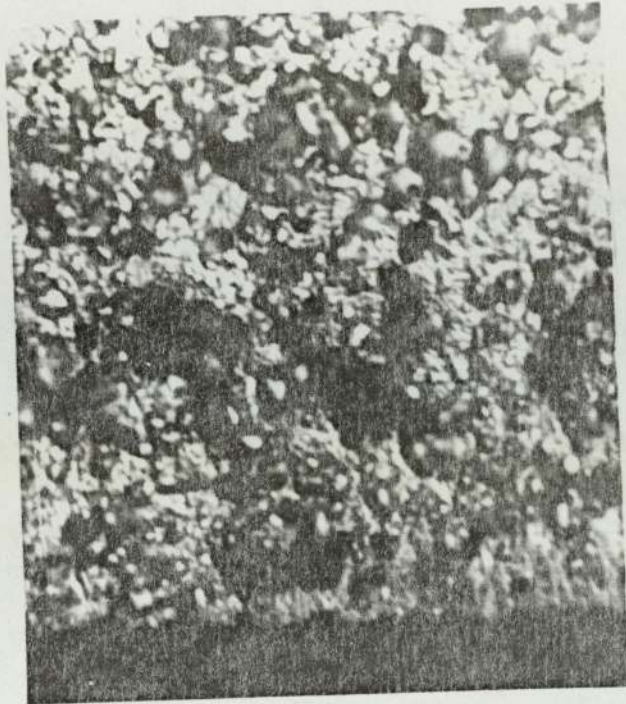


Fig 8.13 The effect of ceramic inclusions on the structure of the electrodeposited metal: silicon carbide in copper, transverse section etched in 10% ammonium persulphate. x 130 enlarged x 3.

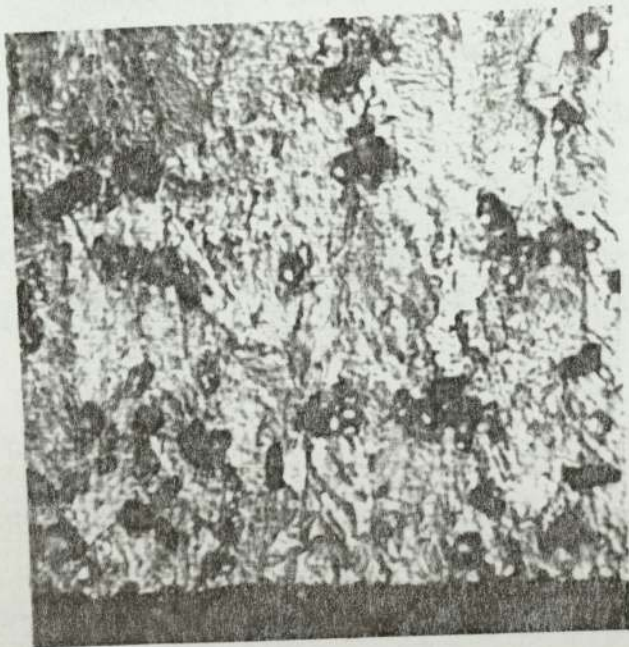


Fig 8.14 The effect of ceramic inclusions on the structure of the electrodeposited metal: chromium diboride in copper, transverse section etched in 10% ammonium persulphate. x 130 enlarged x 3.

Chapter 9. CONCLUSIONS.

When this work was initiated one factor which it was wished to investigate was the importance of the solution pH on the ease of deposition of a solid particle. Previous workers had suggested that the pH of the solution was important in the deposition of particles of certain materials,^{3,21,24} (see 2.1 - 4), particularly lubricants such as graphite and molybdenum disulphide. They suggested that particles of these materials could adsorb hydrogen ions from solutions having low pH, (below 4), thus becoming positively charged.

N.B. That a low pH is not essential for the deposition of all types of particle is well known and much work has been done on deposition from alkaline solutions.^{21,36}

The findings on silicon carbide show no sudden positive increase in the value of the zeta potential as the pH of the solution is lowered. The results suggest that the change of zeta potential with electrolyte concentration is dependent on the total specific bulk conductance, K'_b , of the solution rather than on the particular electrolyte or combination of electrolytes present. The hypothesis of hydrogen ion adsorption onto a particle does not seem justified for silicon carbide, at least in so far as the effect of pH on the zeta potential is concerned. N.B. there could be effects on the cathode surface due to pH but investigation of this was not the object of this work.

We have shown that in the systems which we have studied the change of zeta potential is not determined by the presence of a specific ion or combination of ions but is simply an ionic strength effect.

Electrophoretic transport of particles in the bulk of the solution is negligible compared with hydrodynamic transport, (see 7.2). However, once brought to the fixed portion of the electrochemical double layer on the cathode a positively charged particle can be very rapidly electrophoretically transported through it to the cathode surface, the rate of transport through the double layer becoming greater as the positive charge on the particle is increased.

The results of these electrodeposition experiments showed that mechanical entrapment of particles is most likely to occur on those parts of the cathode surface which are rough or irregular, e.g. in cracks, crevices or troughs in the surface where particles could lie shielded from the effects of the moving solution until keyed into position with metal.

The bond between the metal and the ceramic particle appeared to be mechanical, i.e. the metal mechanically holding the ceramic particle in position in the deposit. No evidence was found which suggested that there was any chemical bond or any intermediate solid phase between the matrix metal and the ceramic inclusion.

Considered together these results suggest that hydrodynamic transport to the vicinity of the cathode followed by electrophoretic transport of particles within the compact portion of the double layer on a cathode and also mechanical entrapment of particles may be significant in the preparation of cermets by electrodeposition.

SUGGESTIONS FOR FUTURE WORK.

Knowledge of the relationship between the following variables would be of value in the more complete understanding of the codeposition process.

1. The effect of current density on ceramic inclusion density in a deposit.
2. The effect of the particle size of a given ceramic on the readiness of inclusion in a given metal.
3. The distribution of ceramic particles relative to physical features such as grain boundaries in the metal.
4. The nature of various ceramics and the effect of their physical characteristics on deposition: factors would include zeta potential, conductivity and type of material e.g. carbide, boride, metal powder, graphite, plastics.

APPENDIX 1.

A1.1 Particle size. Justification of the use of SiC, 280 grit, for streaming.

The material used for the main investigation was silicon carbide of mean particle size 37 microns. The mean pore size in a diaphragm of this powder satisfies the criterion of Neale,⁶³ who said that if zeta potentials were to be calculated from streaming potential measurements using the Helmholtz-Smoluchowski equation then the pore size between the particles must be at least ten times the thickness of the double layer:

The thickness of the double layer is given for a $Z-Z$ electrolyte by the expression Thickness = $(3 \times 10^7 \times |Z| \times C^{\frac{1}{2}})^{-1}$ cm where $|Z|$ is the valency of the ions and C is the molar concentration.⁶⁸ For $|Z| = 1$, a 1M solution will give a double layer thickness of approximately 3×10^{-8} cm,

a 10^{-3} molar solution will give a thickness of approximately 10^{-6} cm,

a 10^{-6} molar solution will give a thickness of approximately 3×10^{-5} cm and

our lowest concentration, $10^{-5}M$, a thickness of approximately 10^{-5} cm.

For close packed spheres of equal size the radius ratio for a tetrahedral site is equal to 0.225.⁶⁹ If the particles composing the diaphragm are considered as spheres the size of a tetrahedral site in a close packed arrangement will be

$$\begin{aligned} &0.225 \times 37 \times 10^{-4} \text{ cm} \\ &= 8 \times 10^{-4} \text{ cm} \end{aligned}$$

As for our most dilute solution the thickness of the double layer is 10^{-5} cm, the ratio of pore size to double layer thickness

$$= \frac{8 \times 10^{-4}}{10^{-5}} \quad : \quad 1$$

which is approximately 100:1

The criterion of Neale is therefore satisfied for our diaphragm material at the solution concentrations used.

A1.2 Conductance of the material.

Silicon carbide has a significant conductance, $0.47 \text{ ohm}^{-1} \text{ cm}^{-1}$ at room temperature;⁷⁰ because of this an exact value for the zeta potential can not be obtained by using the Helmholtz-Smoluchowski equation, even if surface conductance could be neglected, because one of the assumptions made in the establishment of this equation was that the solid phase was a perfect insulator. The value of the zeta potential obtained will therefore not be an absolute value, only a comparative value. As in this work it is comparative values which are required and as other workers⁵⁰ have satisfactorily made streaming measurements on silicon carbide it may be assumed that this material is satisfactory.

APPENDIX II.

A2.1 Calculation of the zeta potential from experimental results.

The apparent zeta potential was calculated by using the Helmholtz-Smoluchowski equation

$$\zeta = \frac{E}{P} \times \frac{4 \pi \eta_0 K'}{D}$$

where E is the streaming potential, P is the applied hydrostatic pressure, η_0 is the coefficient of viscosity of the solvent, K' is the specific conductance of the solution and D is the dielectric coefficient of the solvent.

K' was measured, using a dip-type cell and a Wayne Kerr Universal A.C. bridge, in $\text{ohm}^{-1} \text{cm}^{-1}$. and this value was converted into electrostatic units:

$$1 \text{ ohm}^{-1} \text{cm}^{-1} = 8.9846 \times 10^{11} \text{ esu}$$

P was measured in cm mercury and converted into electrostatic units:

$$1 \text{ cm mercury} = 1.3332 \times 10^4 \text{ dynes cm}^{-2}$$

Calculation of zeta potential was done using an Elliott 803 digital computer, which also plotted graphs of E vs. P. Details of the program are given at the end of this appendix.

A2.2 Variable terms in the Helmholtz-Smoluchowski equation.

A.2.2 - 1 Viscosity.

The viscosity of water changes slightly with addition of electrolyte such that the actual viscosity of the solution,

$\eta = \eta_{\text{rel}} \times \eta_0$ where η_0 is the viscosity of the pure solvent at the same temperature and η_{rel} is given⁷¹ by

$$\eta_{\text{rel}} = 1 + A\sqrt{C} + BC$$

Using this equation the effect of the presence of electrolyte on viscosity of a solution can be calculated. For KCl the constants have the following values⁷²:

A = 0.0052, B = -0.0140, at 25°C, hence for 0.0001 molar KCl at 25°C

$$\eta = \eta_0 (1 + 0.0052 \times 0.01 - 0.014 \times 0.0001)$$

$$\eta = \eta_0 1.0000506$$

The deviation of η from η_0 is thus 0.005%, which is negligible compared with the other errors. It was thus felt to be completely justified to use η_0 in calculations of zeta.

A2.2 - 2 Dielectric coefficient D.

The dielectric coefficient of water changes slightly with addition of electrolyte according to the empirical expression

$D = D_0 - 2 \delta C$ for values of the concentration C from 0.5 to 2.0 molar.

For 1:1 salts δ is approximately = 5 and for 1:2, 2:1 and 1:3 salts the value of δ is generally between 10 and 15.⁷² No value of δ for copper sulphate could be found in the literature, but if it is assumed to be 15 and if, in addition, it is assumed that the expression is valid for low electrolyte concentrations then for a 0.00001 M solution at 25°C

$$D = 78.3 - 2 \times 15 \times 0.00001$$

$$D = 78.2997. \text{ The deviation from } D_0 \text{ is } 0.004\%.$$

Similarly, for a salt concentration of 0.0005M, (the highest used in this work), the expression gives $D = 78.285$.

The deviation from D_0 is 0.2%. It was considered that these deviations were so small, compared with other errors, as to be negligible. (See Appendix VI.)

A2.2 - 3 Specific conductance K'.

In calculations for zeta the specific bulk conductance K'_b is used instead of the true specific conductance K'_s of the liquid in the diaphragm and the value of the zeta potential obtained will thus be low. The results are set out graphically to show the variation of zeta potential with change of the specific conductance of the solution, i.e. as a graph of K'_b vs. ζ .

A.2.2 - 4 Temperature corrections for viscosity and dielectric constant.

Dielectric constant and viscosity both vary with temperature. The value used in calculation of zeta was therefore determined from the literature⁷³ for the temperature of each experiment.

```

C'
COMMENT PROGRAM FOR CALCULATING ZETA POTENTIALS FROM
NG POTENTIAL MEASUREMENTS.P D GROVES/ASTON UNIVERSITY MARCH 1967'
INTEGER SETS,PP,J.POINTS,I.TOP,INT.NO.L.R'
REAL ETA.TOPX.A.KAPPA.D.FACTOR,PO.M.C.ZETA'
INTEGER ARRAY TITLE(1:20)'
ARRAY POINT,P.DELTAE,DELTAP(1:50)'
SWITCH S:=REPEAT'
REAL PROCEDURE SIGMA(X,N)' INTEGER N' ARRAY X'
BEGIN REAL SUM' INTEGER I' SUM:=0'
  FOR I:=1 STEP 1 UNTIL N DO SUM:=SUM+X(I)'
  SIGMA:=SUM'
END OF SIGMA'
PROCEDURE LSQ(Y,X,M,C,N)' REAL M,C' INTEGER N' ARRAY X,Y'
BEGIN REAL DENOM' ARRAY A,R(1:N)' FOR I:= 1 STEP 1 UNTIL N DO
  BEGIN A(I):=X(I)**2' B(I):=X(I)*Y(I)'
  END'
  DENOM:=(N*SIGMA(A,N))-(SIGMA(X,N)**2)'
  C:=((SIGMA(Y,N)*SIGMA(A,N))-(SIGMA(X,N)*SIGMA(B,N)))/DENOM'
  M:=((N*SIGMA(B,N))-(SIGMA(X,N)*SIGMA(Y,N)))/DENOM'
END OF LSQ'
BOOLEAN PROCEDURE N2(N)' VALUE N' INTEGER N'
BEGIN INTEGER COL' SWITCH SS:=L1,L2,FIN'
COL:=+8191'
ELLIOTT(7,0,0,0,0,3,COL)' ELLIOTT(0,5,N,0,4,2,L1)'
ELLIOTT(4,0,L2,0,0,0,0)'
N2:=TRUE' GOTO FIN'
N2:=FALSE'
END OF N2'

```

COMMENT START OF PROGRAM'

```

READER(1)'R:=1' R:=1' INSTRING(TITLE,R)'
READ SETS,ETA,KAPPA.D.TOP,INT.TOPX'
FACTOR:=4*3.1416*8.9816**2/1.5332'
SETORIGIN(1000,200,800/TOP,3)'
AXES(.2,TOP/INT,(TOPX-1.6)/.2,0,INT,0)'
MOVEPEN(1,TOP-TOP/20)'PLOTTER(20,1)'R:=1'OUTSTRING(TITLE,R)'
MOVEPEN(1,TOP-TOP/12)'
IF N2(1) THEN PRINT £MOD.? ELSE PRINT £ORIG.?'
PLOTTER(10,1)'
FOR A:=2 STEP 1 UNTIL TOPX DO
BEGIN MOVEPEN(A-1.75,-TOP/50)'
  PRINT ALIGNED(2,1).A
END'
MOVEPEN(1.5,-TOP/20)'PLOTTER(15,1)'PRINT £DELTA P?'
PLOTTER(10,1)'
FOR I:= 0 STEP TOP/INT UNTIL TOP DO

```

```

BEGIN MOVEPEN(-.4,I)'
  PRINT DIGITS(4),I
END'
MOVEPEN(-.4, TOP/2)'
PLOTTER(15,3)'PRINT #DELTA E?'
PUNCH(1)'PRINT #L3S2D?'R:=1'OUTSTRING(TITLE,R)'
IF N2(1) THEN PRINT #L2S18?MODIFIED DATA?
ELSE PRINT #L2S18?ORIGINAL DATA?'
FOR J:= 1 STEP 1 UNTIL SETS DO
  BEGIN READER(1)'READ P0,POINTS'
  FOR I:= 1 STEP 1 UNTIL POINTS DO
    BEGIN READ P(I),DELTA E(I)'
      DELTAP(I):= *(P(I)-P0)
    END'
  IF N2(1) THEN
    BEGIN READER(2)'READ NO'PP:=POINTS'
    FOR I:= 1 STEP 1 UNTIL NO DO
      BEGIN READ POINT(I)'
        IF POINT(I)=PP THEN POINTS:=POINTS-1 ELSE
          BEGIN FOR L:=POINT(I)-I+2 STEP 1 UNTIL POINTS DO
            BEGIN DELTAP(L-1):=DELTAP(L)'
              DELTAE(L-1):=DELTA E(L)'
            END'
          POINTS:=POINTS-1
        END
      END
    END
  END'
  LSQ(DELTAE,DELTAP,M,C,POINTS)'
  ZETA:=M*ETA*KAPPA*FACTOR/D'ZETA:=M*ETA*KAPPA*FACTOR/DZETA:=M*ETA*
  PUNCH(1)'PRINT #L2S10?SET?,SAMELINE,DIGITS(2),J,ALIGNED(3,3),
  #L2?SLOPE=?*M.#L?INTERCEPT=?*C.#L?ZETA=?*ZETA'
  MOVEPEN(0,1.6*M+C)'
  DRAWLINE(TOPX-1.6, TOPX*M+C)'
  FOR I:=POINTS STEP -1 UNTIL 1DO
    BEGIN MOVEPEN(DELTAP(I)-1.6,DELTA E(I)'
      CENCHARACTER(J)
    END'IF J LESS SETS THEN
  BEGIN PUNCH(3)'PRINT #L?PEN CHANGE?'WAIT
  D'
  END'
  PLOTTER(15,1)'
  MOVEPEN(TOPX-1.4,3*TOP/4)'
  PRINT#SET SYMBOL?'
  PLOTTER(10,1)'
  FOR I:= 1 STEP 1 UNTIL SETS DO
    BEGIN MOVEPEN(TOPX-1.4,(3*TOP/4.1)-(I*TOP/50))'
      PRINT DIGITS(2),I'
      MOVEPEN(TOPX-1,(3*TOP/4.1)-(I*TOP/50))'
      CENCHARACTER(I)
    END'PUNCH(3)'PRINT #L?NEXT DATA?'
    WAIT'MOVEPEN(TOPX+1.0)'RESTART
  END OF PROGRAM'
  END OF PLOTTER PACKAGE'

```

APPENDIX III

DATA LAYOUT FOR CALCULATION OF ZETA POTENTIALS.

Calculations were carried out using an Elliott 803 digital computer; the program print-out is shown in appendix II.

The data layout used was as follows:

heading

number of sets of data

viscosity of the solution

specific conductance of the solution

dielectric constant of the solution

highest value of the streaming potential (this must be an integral value)

number of divisions on the streaming potential axis
(this must be an integer)

the highest value of the applied pressure (this must be divisible by 0.2.)

(These last three figures are required by the graph-plotter.)

This general information is followed by this additional information for each set of data in turn:

manometer zero reading

number of readings in each set of data.

Lastly the pressure vs streaming potential figures are listed in columns.

A3.1 Headings for each group of data.

The heading was chosen such that it included a "fingerprint" description of the particular diaphragm, the composition of the solution and its concentration.

A3.1 - 1. The diaphragm was identified according to the material of which it is made and also according to which particular diaphragm it is, e.g. the ninth diaphragm of silicon

carbide was given the label SIC9.

A3.1 - 2 The components of the solution were given in terms of chemical symbols, e.g. a solution containing nickel and potassium ions is distinguished by the symbols NIK, (only upper case letters were available on the computer).

A3.1 - 3 The composition of the solution was given in terms of the relative molar quantities of each of the components, e.g. a solution containing half as much potassium ion as nickel ion would be distinguished by the symbols ONE HALF NIK.

A3.1 - 4 The concentration of each solution was identified by a number between 1 and 4:

Number 1 indicated a concentration of $0.000008 \text{ g ion l}^{-1}$

2 indicated a concentration of $0.000032 \text{ g ion l}^{-1}$

3 indicated a concentration of $0.000128 \text{ g ion l}^{-1}$

4 indicated a concentration of $0.000512 \text{ g ion l}^{-1}$

A particular heading may therefore be readily interpreted without need of further reference, e.g. SIC9/ONE HALF NIK/2 would mean that silicon carbide diaphragm number 9 was streamed with a solution containing nickel and potassium ions in the ratio of one part Ni^{++} to half part of K^+ and having a nickel ion concentration of $0.000032 \text{ g ions l}^{-1}$.

APPENDIX IV

STATISTICAL TREATMENT OF EXPERIMENTAL RESULTS

Example of a calculation of confidence limits.

Consider a sample of three points 12, 16, 20.

The unbiased estimate of the population mean in this case

$$= \frac{12 + 16 + 20}{3} \text{ which is the Sample Mean}$$
$$= 16$$

Range of the sample $20 - 12 = 8$

Estimate of the standard deviation of the whole population

$$= \text{Range of the sample} \times a_3$$
$$= 8 \times 0.5908$$
$$= 4.73$$

Estimate of standard deviation of sample means

$$= \frac{4.73}{3}$$
$$= 2.72$$

95% confidence limits for the population mean:

Sample Mean $\pm t_2$ x standard deviation of sample mean

$$= 16 \pm 4.3 \times 2.72$$
$$= \underline{\underline{16 \pm 11.6}}$$

a_3 is a factor relating the range to the standard deviation as a function of the number of items in the sample.

t_2 is "Student's" t variate with two degrees of freedom.

Factors a_3 and t_2 were obtained from "Cambridge Elementary Statistical Tables".

Appendix V.

EXPERIMENTAL RESULTS.

A5.1 Series SIC5.

Title	K'_b	ξ	ξ_{mean}	Range	Limits of variation for 95% confidence
KCL/1	1.56	-7.80 -7.63 -7.07	-7.50	0.73	1.07
KCL/2	4.45	-8.10 -8.39 -8.18	-8.22	0.29	0.425
KCL/3	17.5	-6.67 -6.77 -6.82	-6.75	0.15	0.220
KCL/4	68.4	-4.78 -4.92 -4.84	-4.85	0.14	0.205
H/1	2.95	-9.99 -9.59 -9.22	-9.6	0.77	1.13
H/2	11.3	-7.45 -7.48 -7.44	-7.46	0.04	0.059
H/3	45.9	-3.57 -3.49 -3.50	-3.52	0.06	0.088
H/4	183	-1.68 -1.46 -1.79 -1.78	-1.68	0.33	0.255
CU/1	3.04	-23.10 -22.35 -21.20	-22.22	1.90	2.78
CU/2	7.83	-17.70 -17.05 -16.11	-16.95	1.59	2.33

Title	K'_b	ζ	ζ_{mean}	Range	Limits of variation for 95% confidence
CU/3	30.8	-11.81 -11.6 -11.25	-11.55	0.56	0.820
CU/4	110	-6.57 -6.50 -6.30	-6.46	0.78	0.396
EIGONEHCU/1	2.72	-9.17 -8.69 -8.39	-8.75	0.78	1.15
EIGONEHCU/2	9.32	-7.46 -7.44 -7.19	-7.36	0.27	0.396
EIGONEHCU/4	127.2	-4.17 -3.78 -3.82	-3.92	0.39	0.425
QTRONEHCU/1	2.65	-5.83 -5.56 -5.56	-5.50	0.18	0.264
QTRONEHCU/2	9.56	-4.68 -4.67	-4.68	0.01	0.079
QTRONEHCU/3	38.5	-3.19 -3.05 -2.96	-3.07	0.23	0.337
QTRONEHCU/4	153	-2.47 -2.29	-2.38	0.18	1.42
HALFONEHCU/1	3.77	-7.45 -6.96 -6.90	-7.10	0.55	0.805
HALFONEHCU/2	13.3	-4.93 -4.77 -4.86	-4.85	0.16	0.324
HALFONEHCU/3	52.4	-3.34 -3.38	-3.36	0.04	0.316

Title	K'_b	ζ	ζ mean	Range	Limits of variation for 95% confidence
HALF ONE HCU/4	194	-1.78	-1.79	0.01	0.79
ONEONEHCU/1	4.58	-6.90	-6.87	0.18	0.264
		-6.95			
		-6.77			
ONEONEHCU/2	17.1	-4.03	-4.10	0.12	0.176
		-4.15			
		-4.11			
ONEONEHCU/3	74.6	-2.59	-2.53	0.14	0.205
		-2.56			
		-2.45			
ONEONEHCU/4	287	-2.02	-1.84	0.31	0.454
		-1.71			
		-1.79			
ONEHALFHCU/1	3.95	-8.03	7.96	0.18	0.264
		-8.01			
		-7.85			
ONEHALFHCU/2	14.6	-4.66	-4.63	0.08	0.117
		-4.65			
		-4.58			
ONEHALFHCU/3	58.5	-2.10	-2.14	0.09	0.132
		-2.19			
		-2.13			
ONEHALFHCU/4	278	-1.89	-1.91	0.26	0.381
		-1.79			
		-2.05			
ONEQTRHCU/1	3.33	-7.68	-7.49	0.35	0.563
		-7.45			
		-7.33			
ONEQTRHCU/2	13.7	-5.45	-5.52	0.12	0.176
		-5.57			
		-5.55			

Title	K'_b	ζ	ζ mean	Range	Limits of variation for 95% confidence
ONEQTRHCU/3	55.4	-2.88	-2.86	0.11	0.161
		-2.90			
		-2.79			
ONEQTRHCU/4	216	-1.46	-1.56	0.19	1.50
		-1.65			
ONEEIGHCU/1	3.68	-11.71	-10.65	1.05	1.54
		-10.59			
		-9.66			
ONEEIGHCU/2	12.9	-6.54	-6.54	0.01	0.015
		-6.54			
		-6.53			
ONEEIGHCU/3	51.6	-3.39	-3.48	0.34	0.498
		-3.36			
		-3.70			
ONEEIGHCU/4	201	-1.64	-1.67	0.38	0.557
		-1.88			
		-1.50			

A5.2 Series SIC 6.

Title	K'_D	ξ	ξ mean	Range	Limits of variation for 95% confidence
SIC6/CU/1	2.23	-17.6 -16.9 -16.6	-17.03	1.0	1.47
SIC6/CU/2	7.18	-16.9 -16.7 -16.7	-16.87	0.2	0.293
SIC6/CU/3	26.9	-13.1 -13.5 -13.1	-13.2	0.4	0.586
SIC6/CU/4	99.5	-9.20 -9.03 -8.87	-9.03	0.33	0.484
SIC6/H/1	2.83	-17.5 -17.2 -17.1	-17.27	0.4	0.586
SIC6/H/2	11.4	-16.87 -17.05 -16.43	-16.78	0.62	0.908
SIC6/H/3	45.9	-13.30 -12.48 -13.22	-13.00	0.82	1.23
SIC6/H/4	184.4	-10.90 -11.28 -10.25	-10.81 -10.81	1.03 1.03	1.51
SIC6/CU/B/1	2.06	-9.96 -9.46 -9.21	-9.54	0.75	1.11
SIC6/CU/B/2	7.36	-11.63 -11.9 -11.39	-11.64	0.51	0.747

Title	K'_b	ξ	ξ mean	Range	Limits of variation for 95% confidence
SIC6/CU/B/3	27.5	-9.58 -9.64 -9.56	-9.59	0.08	0.117
SIC6/CU/B/0.001024M 183		-6.78 -7.49 06.05	-6.77	1.44	2.11
SIC6/CU/C/1	2.06	-9.68 -9.32 -9.20	-9.40	0.48	0.703
SIC6/CU/C/2	7.29	-11.13 -10.62 -10.71	-10.82	0.41	0.601
SIC6/CU/C/3	27.8	-8.90 -8.99 -9.15	-9.01	0.25	0.366
SIC6/CU/C/4	100.5	-7.03 -6.40 -6.58	-6.67	0.63	.923

A5.3 Series SIC 7

Title	K'_b	ζ	ζ mean	Range	Limits of variation for 95% confidence
SIC7/CU/1	2.28	-20.47	-19.79	1.15	1.69
		-19.32			
		-19.57			
SIC7/CU/2	7.53	-21.63	-21.56	0.13	1.91
		-21.55			
		-21.50			
SIC7/CU/3	27.7	-17.05	-17.09	0.08	1.17
		-17.13			
		-17.08			
SIC7/CU/4	101.5	-10.94	-10.84	0.20	0.293
		-10.74			
		-10.83			

A5.4 Series SIC8.

Title	K'_b	ζ	ζ_{mean}	Range	Limits of variation for 95% confidence
SIC8/CU/1	2.28	-21.90 -22.04 -22.28	-22.07	0.38	0.411
SIC8/CU/2	7.1	-25.10 -25.14 -25.14	-25.13	0.04	0.059
SIC8/CU/3	27.6	-19.95 -19.94 -19.94	-19.94	0.01	0.015
SIC8/CU/4	96.6	-12.77 -12.79 -13.00	-12.85	0.23	0.337
SIC8/H/1	3.00	-27.00 -27.56 -28.59	-27.72	1.59	2.34
SIC8/H/2	11.6	-36.05 -37.41 -37.40	-36.95	1.36	1.99
SIC8/H/3	46.1	-30.52 -30.00 -30.70	-30.41	0.70	1.03
SIC8/H/4	182.2	-22.82 -22.87 -18.29	-21.33	4.58	6.71
SIC8/CU/B/1	2.15	-18.05 -18.08 -18.39	-18.17	0.34	0.498
SIC8/CU/B/2	7.49	-22.74	-22.61	0.40	0.587

Title	K'_b	ζ	ζ mean	Range	Limits of variation for 95% confidence
		-22.75			
		-22.35			
SIC8/CU/B/3	27.3	-17.90	-18.03	0.20	0.293
		-17.90			
		-18.10			
SIC8/CU/B/4	99.5	-12.10	-12.04	0.10	0.147
		-12.03			
		-12.00			

A5.5 Series SIC 9

Title	K'_b	ζ	ζ mean	Range	Limits of variation for 95% confidence
ONEEIGNIK/1	2.87	-19.30	-18.59	1.38	2.02
		-18.54			
		-17.92			
ONEEIGNIK/2	8.16	-21.18	-21.04	0.28	0.410
		-21.05			
		-20.90			
ONEEIGNIK/3	30.1	-19.65	-19.79	0.21	0.308
		-19.86			
		-19.85			
ONEEIGNIK/4	112	-16.60	-16.5	0	0
		-16.50			
ONEQTRNIK/1	2.36	-16.49	-15.72	1.18	1.73
		-15.31			
		-15.37			
ONEQTRNIK/2	8.68	-21.25	-21.09	0.30	0.440
		-21.06			
		-20.95			
ONEQTRNIK/3	32.6	-20.06	-20.02	0.11	0.161
		-20.05			
		-19.95			
ONEHALFNIK/1	2.74	-17.43	-17.04	0.59	0.865
		-16.84			
		-16.85			
ONEHALFNIK/2	10.35	-21.97	-21.58	0.71	1.04
		-21.50			
		-21.26			
ONEHALFNIK/3	39.1	-20.92	-20.84	0.16	0.235
		-20.85			
		-20.76			

Title	K'_b	ξ	ξ mean	Range	Limits of variation for 95% confidence
ONEHALFNIK/4	143.5	-17.08	-16.48	1.52	2.23
		-16.80			
		-15.56			
ONEONENIK/1	3.20	-18.23	-18.00	0.53	0.777
		-18.07			
		-17.70			
ONEONENIK/2	11.67	-22.11	-22.10	0.06	0.088
		-22.07			
		-22.13			
ONEONENIK/3	47.2	-21.53	-21.50	0.14	0.205
		-21.41			
		-21.55			
ONEONENIK/4	165	-18.21	-18.0	0.41	0.601
		-17.99			
		-17.80			
HALFONENIK/1	2.09	-16.33	-15.94	0.70	1.03
		-15.86			
		-15.63			
HALFONENIK/2	8.0	-22.82	-22.64	0.31	0.454
		-22.60			
		-22.51			
HALFONENIK/3	31	-22.92	-22.90	0.07	0.103
		-22.92			
		-22.85			
QTRONENIK/1	2.01	-15.65	-15.81	0.47	0.689
		-16.12			
		-15.65			

Title	K_b^t	ζ	ζ mean	Range	Limits of variation for 95% confidence
QTRONENIK/2	6.65	-23.83 -23.81 -23.73	-23.79	0.10	0.147
QTRONENIK/3	24.7	-28.03 -26.66 -26.96	-27.22	1.37	2.01
KCL/1	1.71	-13.98 -14.82 -13.73	-14.18	1.09	1.60
KCL/2	5.01	-23.47 -22.65 -21.71	-22.61	1.76	2.58
KCL/3	18.70	-26.29 -25.71 -25.57	-25.86	0.72	1.06
KCL/4	71.6	-24.42 -24.89 -24.33	-24.55	0.56	0.821
N12/1	2.17	-9.00 -9.01 -9.00	-9.00	0.01	0.015
N12/2	7.35	-15.72 -15.84 -15.65	-15.74	0.19	0.279
N12/3	27.41	-18.15 -18.22 -17.97	-18.11	0.25	0.367
N12/4	101.4	-16.24	-16.44	0.83	1.22

Title	K'_b	ξ	ξ mean	Range	Limits of variation for 95% confidence
		-16.96			
		-16.13			
KS2/1	1.33	-9.62	-9.44	0.28	0.410
		-9.34			
		-9.35			
KS2/2	4.57	-20.29	-20.32	1.14	1.67
		-20.90			
		-19.76			
KS2/3	17.12	-30.02	-30.08	0.42	0.616
		-30.22			
		-29.90			
EIGONENIK/1	1.50	-14.41	-14.08	0.60	0.88
		-14.03			
		-13.81			
EIGONENIK/2	5.81	-25.37	-25.07	0.72	1.06
		-25.20			
		-24.65			
EIGONENIK/3	21.34	-28.58	-28.21	0.96	1.41
		-27.62			
		-28.44			
N1/1	3.54	-24.29	-23.08	1.81	2.65
		-22.48			
		-22.48			
N1/2	8.27	-26.80	-26.83	0.80	1.17
		-26.44			
		-27.24			

Title	K'_b	ξ	ξ_{mean}	Range	Limits of variation for 95% confidence
N1/3	30.92	-27.68	-27.27	0.85	1.25
		-27.31			
		-26.33			
N1/4	111	-21.68	-21.44	1.31	1.92
		-21.98			
		-20.67			
KS/1	1.77	-20.48	-19.85	1.00	1.47
		-19.59			
		-19.48			
KS/2	5.5	-29.21	-29.85	1.27	1.86
		-30.43			
		-29.86			
KS/3	18.9	-33.62	-33.77	0.39	0.572
		-33.67			
		-34.01			
KS/4	72.6	-30.73	-30.22	0.69	1.01
		-30.20			
		-30.04			

A5.6 Series CRB2.

Title	K'_D	ξ	ξ mean	Range	Limits of variation for 95% confidence
CRB2/CU/1	2.33	1.503	1.505	0.025	0.037
		1.518			
		1.493			
CRB2/CU/2	8.16	4.25	4.92	1.37	1.06
		3.60			
		3.22			
		4.59			
CRB2/CU/3	30.8	11.88	11.72	0.38	0.557
		11.50			
		11.77			
CRB2/CU/4	110.5	21.66	23.43	4.65	3.59
		21.66			
		24.10			
		26.31			
CRB2/H/1	2.05	0.710	0.663	0.116	0.170
		0.594			
		0.684			
CRB2/H/2	11.3	5.44	5.64	0.63	0.923
		5.42			
		6.05			
CRB2/H/3	47.6	10.59	10.29	0.59	0.864
		10.00			
		10.28			
CRB2/H/4	187	11.27	11.52	0.96	1.41
		12.05			
		12.23			

APPENDIX VI

CALCULATION OF MAXIMUM EXPERIMENTAL ERROR.

Specific conductance K'_d .

Drift on measurement at low values up to 0.1 on 2.5 $\pm 4\%$
Drift on measurement at higher values: up to 2.0 on 100 $\pm 2\%$

Temperature

Errors in reading of the thermometer: 0.2°C would give an error:

in D of ± 0.1 on 80 $\pm 0.1\%$

in \circ of ± 0.05 on 10 $\pm 0.5\%$

Pressure P.

On the inclined scale, 1 mm in 30 mm for P = 1 $\pm 3\%$

1 mm in 180 mm for P = 6 $\pm 0.5\%$

Streaming potential E.

Precision of reading of the electrometer when using dilute

solutions 10 in 1000, $\pm 1\%$

in more concentrated solutions, 0.4 in 10 $\pm 4\%$

Permeability.

The use of non compressible granules should have given a constant permeability to the diaphragm. It was sometimes noticed that the streaming activity of a diaphragm decreased with successive runs with the same solution. This was attributed to an increasing closeness of packing in the diaphragm giving rise to higher surface conductance. The fall in streaming activity was particularly large in SIC 9/ONE QTR NIK/1 and SIC 9/ ONE HALF NIK/1

Error due to change in permeability $\pm 8\%$

Total error $= \pm 19.6\%$

N.B. Relative errors are added when the quantities are to be multiplied or divided. A theoretical justification of this is given, for example, by Butler and Kerr.⁷⁵

It is possible that slight errors could arise from the following factors but these were considered to be negligible for the

reasons stated.

Polarisation of cells

This was considered to be negligible as when streaming pressure was reduced to zero the emf between the cells fell approximately to zero within about one minutes.

Leaching of potassium chloride from probes.

Leaching would not have reduced the observed streaming potential very greatly as the conductance K'_b of the solution would be little altered by this quantity of KCl. KCl loss from the agar jelly in the ends of the probes could have reduced the sensitivity of emf measurement but this was not noticed in practice.

Mat effects.

Whatman 541 paper was used throughout and any mat effect would therefore be a constant factor. The electrokinetic activity of the mat was measured in the absence of the diaphragm and allowance was made for this in all calculations.

CO₂ uptake by water.

This was prevented, during storage, by a soda-lime CO₂ trap. While streaming was in progress the solution was exposed to the air as it was considered to be better, as the period of exposure was short, than using a trap which could allow soda-lime dust to enter the solution. At the end of each run the conductance of the remaining liquid in the tank was again measured. The variation in conductance was seldom measurable.

Leaching of salts from the glass.

This was minimised by soaking the glass in acid followed by steaming out. The method was described in 5.2.

Conductance of the diaphragm material.

In the case of SiC and CrB₂ this is appreciable, but constant. See Appendix 1.

Effect of immersion time on streaming activity.

It was found that although streaming activity fell after prolonged immersion in a stationary solution it returned to its previous value after a short time, in the order of five minutes,

under a streaming pressure of about 10 cm of mercury. It was assumed that various materials had been adsorbed by the silicon carbide while standing in contact with the liquid and that these were being washed away from the surface. This result was in contrast to the findings of Lewis.⁵⁰

Graphs of E vs P.

These graphs were drawn by the computer graph-plotter. Instructions to the computer for use of the graph-plotter were included in the Zetacalc program (see appendix II). The computer drew a least-squares straight line through the experimental points. When a graph had been drawn a visual examination showed whether any points were wildly wrong and these could be deleted from the data and the graph redrawn by the computer.

Limits of experimental error.

The total error is, to the nearest whole number $\pm 20\%$.

Appendix VII.

BIBLIOGRAPHY.

1. J.J.Gilman, Scientific American (1967), 217 no 3, 115.
2. D.Fishlock, New Scientist (1966), 29 no 481, 283.
3. G.F.Bidmead, B.S.A. report GRC/G2260 (1964).
4. J.C.Withers, WADD Technical Report (1961).
5. I.Crivelli-Visconti & G.A.Cooper, Nature (1969),
221 no 5182, 754.
6. J.H.Westbrook, Amer. Ceram. Soc. Bull. (1956), 35, 47.
7. L.W.Davies, ASTM (1967), STP 427.
8. D.Cratchley & A.A.Baker, Metallurgia (1964), 69, 153.
9. D.Cratchley & A.A.Baker, Symposium on the contact of hot metal
with glass, Union Scientific Continental Du Verre,
Schwenigen, (1964).
10. G.Economos & W.D.Kingery, J.A.Ceram.Soc. (1953), 36, 403.
11. F.A.Cotton & G.Wilkinson, Advanced Inorganic Chemistry,
1st Ed., Interscience, (1962).
12. C.A.Hauck, J.C.Donlevy & T.S.Shevlin, Wright Air
Development Technical Report (1956), 54.
13. A.G.Thomas, J.B.Huffadine & N.C.Moore, Metallurgical
Reviews (1963), 8, 467.
14. A.Kelly & L.G.Davies, Ibid (1956), 10, 1.
15. D.Cratchley, Ibid (1956), 10, 79.
16. J.C.Withers, Products Finishing (1962), 26 no 11, 62.
17. R.J.Fabian, Materials in Design Engineering (1962), 56, 105.
18. A.E.Grazen, U.S. Patent 3061525.
19. F.K.Sauter, J.Electrochem. Soc. (1963), 110, 557.
20. G.D.Spencely, BISRA Report MW/INT/10,62 (1962).
21. R.V.Williams & P.W.Martin, 6th International Metal
Finishing Conference (1964).
22. R.V.Williams, Electroplating & Metal Finishing (1966).

23. E.C.Kedward & B.Kiernan, Metal Finishing Journal (1967), 117.
24. E.C.Kedward, Unpublished work.
25. G.Isserlis, Private Communication.
26. A.K.Wood, Society of Automotive Engineers Congress, Detroit (1964), 784 A.
27. D.C.Mitchell, I.Mech.E. Conference on Lubrication and Wear (1957), 396.
28. W.Hirst, Ibid, 674.
29. J.K.Lancaster, I.Mech.E. Proceedings (1967-8) 182 pt 1 no 2.
30. A.A.Baker, S.J.Harris & E.Holmes, Metals and Materials, (1967), 211.
31. N.R.Adsit, ASTM (1967), STP 427.
32. J.A.Alexander & W.F.Sturke, ASTM (1967), STP 427.
33. D.W.Pertasek, R.A.Signorelli & J.W.Weeton, ASTM (1967), STP 427.
34. R.G.Shavers & J.C.Withers, 10th Refractory Composites Working Group Meeting, Atlanta (1965).
35. BISRA unpublished work.
36. E.A.Brandes & D.Goldthorpe, Metallurgia (1967), 76 no 457, 195.
37. Udylite "Dur-Ni" process, See J.M.Odekerken, Electroplating and Metal Finishing (1964), 17 no 4, 2.
K.R.Barnett, Metal Progress (1964), 87.
38. W.T.Gunston, Science Journal (Feb 1969).
39. H.von Helmholtz, Wied. Ann. (1879), 2, 337. Translated as Eng. Res. Bull. no 33 (1951), Univ. Michigan.
30. G.Gouy, J.Phys. (1910), 2 no 4, 457.
41. D.L.Chapman, Phil. Mag. (1913), 25, 475.
42. G.Kortüm, Treatise on Electrochemistry, 2nd Ed., Elsevier (1965), 392,401.
43. O.Stern, Z.Electrochem. (1924), 30, 508.

44. D.C.Grahame, Chemical Reviews (1947), 41, 441.
45. D.C.Grahame, Z.Electrochem. (1955), 59, 773.
46. Devanathan, Bockris & Muller, Proc.Roy.Soc. (1963),
A274, 55.
47. M.von Smoluchowski, Bull.Intern.Acad.Sci.Cracovie (1903),
A, 182. Also in Handb.d.Electr.und Magnet., vol II,
Graetz (Ed), Leipzig, (1921), 374.
48. G.Kortüm, Treatise on Electrochemistry, 2nd Ed.,
Elsevier (1965), 424.
49. J.Th.Overbeek & P.W.O.Wijga, Rec.Trav.Chim. (1946),
65, 556.
50. A.F.Lewis, Thesis, Lehigh University (1958).
51. Stock, Bull.Intern.Acad.Sci.Cracovie (1912), A, 635.
52. U.Saxen, Weid. Ann. (1892), 47, 46.
53. P.Mazur & J.Th.Overbeek, Rec.Trav.Chim.(1951), 70, 83.
54. P.W.O.Wijga, Thesis, Utrecht University, (1946).
55. S.Glasstone, Textbook of Physical Chemistry, 2nd Ed.,
Macmillan (1948), 1240.
56. A.J.Rutgers & M.deSmet, T.Far.Soc. (1945), 41, 746.
57. G.Kortüm, Treatise on Electrochemistry, 2nd Ed.,
Elsevier (1965), 405,434.
58. H.Schulze, J.Pract.Chem. (1882), 25 no 2, 431, and Ibid
(1883), 27, 320.
59. W.B.Hardy, Proc.Roy.Soc.(1900), 66, 110 and
Z.Physic.Chem.(1900), 33, 385.
60. E.J.W.Verwey & J.Th.Overbeek, Theory of the Stability
of Hydrophobic Colloids, Amsterdam (1948).
61. F.Fairbrother & H.Mastin, J.C.S.(1924), 125, 2319, 2321.
62. D.R.Briggs, J.Phys.Chem. (1928), 32, 461.
63. S.M.Neale, J.Far.Soc. (1946), 42, 474.
64. J.F.Hazel, J.Electrochem.Soc. (1953), 100, 65.

65. Whatman Technical Bulletin F1, 29.
66. S.Glasstone, Textbook of Physical Chemistry, 2nd Ed.,
Macmillan (1948), 1225.
67. G.A.H.Elton, Proc.Roy.Soc.(1949), A197, 568.
68. P.Delahay, Double Layer and Electrode Kinetics,
Wiley (1965), 44.
69. W.E.Addison, Structural Principles in Inorganic
Compounds, Longmans (1961).
70. R.W.Sears & J.A.Becker, Physical Reviews (1932),40, 1055.
71. Jones et al, J.A.C.S.(1933-40), see G.Kortüm, Treatise
on Electrochemistry, 2nd Ed., Elsevier(1965), 200.
72. R.Parsons, Handbook of Electrochemical Constants,
Butterworths (1959).
73. International Critical Tables, McGraw-Hill (1956).
74. B.E.Conway, Electrode Processes, Ronald Press, N.Y.,(1965).
75. R.Butler & E.Kerr, An Introduction to Numerical Methods,
Pitman (1962), 6.